Non-invasive ultrasound-based cardiovascular imaging in mouse models of atherosclerosis

Julia Grönros

2008

The Sahlgrenska Academy
AT GÖTEBORG UNIVERSITY
Institute of Neuroscience and Physiology

Cover: Illustration of the left coronary artery
made by Sandra Svensson

Julia Grönros
Göteborg 2008
Tryck: Intellecta Docusys AB, V Frölunda 2008
ISBN 978-91-628-7388-2

Till Mamma och Pappa

ABSTRACT

Atherosclerosis is a chronic multi-factorial vascular disease. It generally requires large clinical settings and over many years to study the disease progression in man. Genetically modified mouse models of atherosclerosis have dramatically increased research feasibility within this area. However, for optimal translational studies, it is increasingly important to explore how human-like these atherosclerotic mouse models demonstrate their disease phenotype and respond to established cardiovascular interventions.

The aims of this thesis were to develop and apply *in vivo* translational techniques to study living atherosclerotic mice, with human-relevant disease phenotype.

Color Doppler guided echocardiography and a high-frequency ultrasound biomicroscope were used for imaging of peripheral and coronary artery function and morphology. The potential role of IL-18 in mice was explored in relationship to mouse coronary artery disease. Finally temporal effects of rosuvastatin on cardiovascular phenotype were studied in an ApoE knockout mouse model of atherosclerosis.

This thesis illustrates that it is possible to investigate both central and peripheral atherosclerosis in living mice using ultrasound-based techniques. Our findings may also suggest an important role of IL-18 in late stage atherosclerosis in an advanced model of atherosclerosis. Finally, this particular ApoE knockout mouse model showed time-dependent beneficial cardiovascular effects following rosuvastatin treatment.

The established translational functional and morphological imaging platform in combination with our human-like statin-responding mouse model, provide us with powerful tools for future atherosclerosis research.

TABLE OF CONTENTS

LIST OF PUBLICATIONS

This thesis is based upon the following published papers or manuscripts:

I. **Grönros Julia, Wikström Johannes, Hägg Ulrika, Wandt Birger, Gan Li-ming**
Proximal to middle left coronary artery flow velocity ratio, as assessed using color Doppler echocardiography, predicts coronary artery atherosclerosis in mice.
Arterioscler Thromb Vasc Biol. 2006 May;26(5):1126-31. Epub 2006 Mar 2.

II. **Wikström Johannes, Grönros Julia, Bergström Göran, Gan Li-ming**
Functional and morphologic imaging of coronary atherosclerosis in living mice using high-resolution color Doppler echocardiography and ultrasound biomicroscopy.
J Am Coll Cardiol. 2005 Aug 16;46(4):720-7.

III. **Gan Li-ming, Grönros Julia, Hägg Ulrika, Wikström Johannes, Theodoropoulos Catherine, Friberg Peter, Fritsche-Danielsson Regina**
Non-invasive real-time imaging of atherosclerosis in mice using ultrasound biomicroscopy.
Atherosclerosis. 2007 Feb;190(2):313-20. Epub 2006 May

IV. **Grönros Julia, Wikström Johannes, Berke Zsofia, Andreasson Anne-Christine, Lundin Sofia, Gan Li-ming**
High circulatory interleukin-18 levels are associated with advanced coronary artery atherosclerosis in mice.
Submitted

V. **Grönros Julia, Wikström Johannes, Brandt-Eliasson Ulla, Forsberg Gun-Britt, Behrendt Margareta, Hansson Göran I, Gan Li-ming**
Effects of rosuvastatin on cardiovascular morphology and function in an ApoE knockout mouse model of atherosclerosis.
Submitted

ABBREVIATIONS

ApoE KO	apolipoprotein E knock out
BP	blood pressure
CDE	color Doppler echocardiography
CFR	coronary flow reserve
CFVR	coronary flow velocity reserve
CM	chylomicron
CO	cardiac output
DKO	double knock-out
EDV	end-diastolic volume
EF	ejection fraction
FS	fractional shortening
HDL	high density lipoprotein
HMG-CoA	3-hydroxy-3-methyl-glutaryl coenzyme A
HR	heart rate
IDL	intermediate-density-lipoprotein
IEL	internal elastic lamina
IFN-γ	interferon-gamma
IL-18	interleukin-18
IMT	intima-media thickness
LAD	left artery descending
LCA	left coronary artery
LDL	low density lipoprotein
LDLr	low density lipoprotein receptor
LV	left ventricle
LVM	left ventricular mass
LVM/bw	body weight adjusted left ventricle mass
MLD	minimal lumen diameter
MRI	magnetic resonance imaging
PWT	percentage wall thickness
SAA	serum amyloid A
SV	stroke volume
TG	triglycerides
TNF-α	tumour necrosis factor-alpha
UBM	ultrasound biomicroscope
VLDL	very low density lipoprotein
Vmid	velocity in middle part of LCA
Vprox	velocity in proximal part of LCA
Vratio	velocity ratio
VTI	velocity time integral
WT	wall thickness

INTRODUCTION

Cardiovascular disease

Cardiovascular disease is the comprehensive name for disorders in the circulatory system. This includes high blood pressure, coronary heart disease, heart failure, stroke and congenital cardiovascular defects. In Sweden approximately 60 men and 25 women die every day from cardiovascular disorders[1]. Coronary artery atherosclerosis is the main cause of cardiovascular mortality and morbidity. Atherosclerosis is a complex, multifactorial disease, where a dysfunctional endothelium, lumen-narrowing plaque formation, plaque inflammation and plaque rupture, are recognized as major features associated with cardiovascular events. Without doubt, however, hypercholesterolemia and inflammation are major components that trigger atherosclerosis[2].

Atherosclerosis – an inflammatory process

During the past decade, the theory of atherosclerosis as a low-grade inflammatory disease of the larger arteries has become more and more accepted. Hypercholesterolemia, smoking, high blood pressure and diabetes are believed to be risk factors for the disease. An early step in the atherosclerotic process is believed to involve the endothelium, the layer closest to the circulation in the artery, which becomes permeable to circulating lipoproteins that subsequently accumulate in the intima. Once the endothelium is activated, the expression of adhesion molecules is up-regulated on the endothelial surface[3]. Circulating platelets and leukocytes (for example monocytes and T lymphocytes) may bind to adhesion receptors and infiltrate from the circulation into the intima as a response to injury. The critical step for the atherosclerotic development is when the infiltrated monocytes are exposed to macrophage colony-stimulating factor (MCS-factor), produced by the inflamed endothelium. This can stimulate monocytes differentiation into macrophages that start to engulf the already

present oxidized low-density lipoproteins (LDL) under the intima and transform themselves into foam cells. Macrophages in turn present T lymphocyte-activating antigens on their surface that activate the T cells. T cells are one of the cell types always present in all kinds of tissue, prepared for an immune response. Together, the macrophages and T lymphocytes give rise to the initial fatty streak formation that precedes more advanced atherosclerotic plaques. The activation of T cells induces a cascade of cytokines. As fatty streaks progress, ligand-receptor processes on T cells may promote cytokine expression of interferon-gamma (IFN-γ) and tumour necrosis factor-alpha (TNF-α). IFN-γ is a macrophage stimulating cytokine, which activates macrophages to express TNF-,α and interleukin-1 (IL-1), which can boost the inflammation. Smooth muscle cells are recruited from the media and produce collagen that build up the fibrous cap, which separates the lesion from the lumen. As the plaque grows it will intrude into the artery lumen and may eventually prevent blood flow. As the plaque gets more advanced, metalloproteinases released by macrophages may degrade the fibrous cap and reduce the stability of the atherosclerotic lesion, thus making it more rupture prone. If a plaque ruptures, thrombotic agents are exposed to the circulation and form a thrombus. This thrombus can occlude the vessel and prevent downstream blood flow or follow the blood stream to a narrower vessel site. Both the lumen-narrowing plaque growth and the thrombus-formation following plaque rupture, have a strong relation to myocardial infarction and stroke[4, 5, 6].

Interleukin-18 and inflammation

Macrophages and T cells, prominent in the intima, express a large number of proinflammatory cytokines[7,6]. A cytokine functionally related to the IL-1 family[8], interleukin-18 (IL-18), is a pro-inflammatory cytokine that acts to induce interferon-γ[9]. Recent findings suggest that IL-18 is expressed by vascular endothelial cells, smooth muscle cells and by macrophages of human plaques[10]. High levels of IL-18 in the blood are suggested to play a role at a

late stage in the progression of atherosclerosis[11]. In mice, exogenously administered IL-18 has been shown to accelerate the progression of atherosclerosis in ApoE KO mice[12]. In addition, atherosclerosis was reduced in the aortic root in an ApoE KO mice model that was simultaneously deficient for the IL-18 gene[13].

Lipoproteins

Nearly all dietary fat required for energy production, both vegetable fats stored in seeds and animal fats stored in adipocytes, consists of triglycerides. Cholesterol, one of the crucial components of cell membranes and the precursor of some hormones is primarily produced by the liver (and intestines), but can also originate from dietary intake. Both triglycerides and cholesterol are insoluble in water and therefore also in the blood. Consequently they are transported in the circulation by lipoproteins. The main groups of lipoproteins are chylomicrons, very-low-density lipoproteins, intermediate-density lipoproteins, low-density lipoproteins and high-density lipoproteins. The lipoproteins differ in terms of size, density, lipid composition and apolipoprotein content. They consist of a core with TG and CE surrounded by a water-soluble layer of the specific apolipoprotein (Apo A1, A2, A4, Apo B48, B100, Apo C1, C2, C3 or Apo E), cholesterol and phospholipids[14, 15]. The content of the core differs depending on the lipoproteins nature. LDL and HDL are the main carriers of cholesterol whilst chylomicron and VLDL carry mainly triglycerides.

The lipoproteins are also distinguished by their main pathways:
Chylomicrons (CM) transport dietary triglycerides from the intestines to peripheral tissue such as muscles, heart and adipose tissue where they are used as energy in the form of free fatty acids or re-estrified for storage. The chylomicron remnants are transported to the liver for clearance from the circulation or to become surface material for the HDL particles. On the surface of the liver cells LDL receptors binds to apolipoprotein E on the surface of chylomicron remnants. Very-low-density-lipoproteins

(VLDL) rich in triglycerides are secreted from the liver to the circulation and like the chylomicrons incorporated in peripheral tissue as energy source. The remnant particles called intermediate-density-lipoproteins (IDL) are transported either back to the liver or transformed into low-density-lipoproteins (LDL) particles in the plasma. The main purpose for the LDL particles is to transport cholesterol to peripheral tissue. High-density-lipoproteins (HDL) on the other hand transport cholesterol from the peripheral tissue to the liver for excretion in the form of bile in a process called reverse cholesterol transport. This is the reason for naming the LDL the "bad cholesterol" since it transports cholesterol to peripheral tissue, including the arteries, which is pro-atherogenic. HDL is named the "good cholesterol" since it transports cholesterol from the peripheral tissue such as the arteries and thus may reduce atherosclerosis[16, 17].

Statins

The development of pharmaceutical treatment that modifies circulating lipoprotein levels and protects against atherosclerosis is of major interest for atherosclerotic prevention. One type of treatment already available is statins. The main effect of statins is the inhibition of hydroxymethylglutaryl-Coenzyme A (HMG-CoA) reductase, the enzyme controlling the rate-limiting step of the liver cholesterol biosynthesis. As the endogenous biosynthesis of cholesterol is inhibited in the liver expression of LDL receptors is up-regulated on the hepatic cell surface. This leads to increased uptake of cholesterol-containing LDL particles from the circulation, which lowers the LDL cholesterol levels. Statins have also shown a beneficial effect by increasing HDL levels. There might also be pleiotropic effects from statins in terms of improving endothelial function, lowering systemic and local inflammation, and decreasing atherosclerotic plaque growth[18, 19].

Mouse models of atherosclerosis

The normal wild-type mouse does not develop atherosclerosis, mainly because of their high levels of the circulating protective HDL. Since the mouse genome became completely mapped a few years ago (Collins and Lander 2002) the possibilities have increased for knocking out or inserting new genes. This effort became important in the development of mouse models resembling human diseases. When creating a knockout mouse model, cultured embryonic mouse stem cells with a specific gene in the genome disrupted, are used. These stem cells are placed in a fertilized egg and implanted into the uterus of the host mother mouse. Genetically modified mice with disturbances in the lipid profile or inability of lipid clearance from the circulation, for example the ApoE KO and LDLr KO mouse are important in the preclinical field of atherosclerosis research. These mice spontaneously develop hypercholesterolemia and atherosclerosis in several vascular beds, accelerated when they are fed a high-fat and/or high-cholesterol diet[20-22].

Coronary arteries

From the aortic sinus, two major branches of descending coronary arteries arise; the left coronary artery (LCA) supplying the left ventricle and septum with blood and the right coronary artery supplying the right ventricle with blood[23] . Filling of the coronary arteries is affected by two major factors; the contraction of the ventricles and the aortic pressure. During the diastolic phase of the cardiac cycle when the ventricles are relaxed and the aortic pressure is high is when the main flow can rise in the coronary arteries. Regulation of the coronary blood flow is dependent on the cardiac metabolic demand. Under resting conditions the coronary arteries are autoregulated. With autoregulation changes in blood pressure or flow cause the arteries to either constrict or dilate to compensate. Thus, myocardial cells have extremely high oxygen consumption. 65% of the oxygen carried out at rest is

extracted and used compared to 25% in other tissue cells. Consequently, the only way to increase the oxygen supply at emerging need is through an increase in the blood flow[24]. At increased oxygen demand, for example during exercise or in a clinical stress test using vasodilators such as adenosine, local carbon dioxide accumulation stimulates the release of nitric oxide from the endothelial layer. This metabolic mechanism relaxes the smooth muscle cells of the arteries and thereby increase blood flow[25]. The proximal parts (in humans a diameter between 120-150 μm) of the coronary arteries are sensitive to flow-mediated vasodilatation whilst the smaller arterioles (diameter 30-60 μm) are under myogenic control and the smallest (diameter <30 μm) under metabolic control[25, 26] .

Coronary artery atherosclerosis

As mentioned above, coronary artery atherosclerosis is the major cause of death in the Western world[1] and has been shown to be the strongest predictor of cardiovascular events[27]. The development of coronary artery atherosclerosis is dependent on several factors. In addition to the regular risk factors such as hypercholesterolemia and inflammation the coronary arteries are also under constant movement of the myocardium. In general, atherosclerotic lesions tend to appear where the blood flow is oscillatory or turbulent[28, 29].

There is an emerging need for methods to investigate both morphology and function of the coronary arteries. Two different approaches to accomplish this are;
- The velocity ratio approach
- The concept of coronary flow velocity reserve

Velocity ratio

The flow velocity of a fluid over a narrow site in a pipe or hose causes the velocity to rise, notable by the increase in sound. In an artery affected by atherosclerosis the lumen diameter might be narrowed, referred to as a stenosis. This leads to an increase in

velocity over that specific site. A stenosis can lead to decreased blood flow and oxygen supply to the more distal arteries[30]. This event can be applied clinically when investigating coronary artery atherosclerosis. Using color Doppler guided echocardiography it is possible to measure flow velocity "in stenosis" and after the vascular narrowing, "post stenosis". The ratio between these two sites indicates if there is a narrowing of the lumen at one of the sites.

Coronary flow velocity reserve, CFVR

Coronary flow velocity reserve (CFVR) and the volumetric counterpart coronary flow reserve (CFR) are both measurements of the heart's capacity to respond to increased oxygen demand, needed for example during exercise[31, 32]. Both CFVR and CFR can be tested clinically in a stress test using vasodilatating substances. The coronary flow reserve is calculated as the hyperemic value divided by the basal value. The normal ranges for CFR in humans are between 3.5 and 5 while a CFR ratio below 2 is considered as pathologic. Both the CFVR and the CFR can be used in man to investigate coronary artery stenosis and minimal lumen diameter[33, 34] . There are several parameters that could affect CFR. Vassalli et al. summarizes several parameters to take into consideration, such as diffuse coronary artery disease, small-vessel disease, regional variations of myocardial flow, endothelial dysfunction and left ventricle hypertrophy[35]. Heart rate, blood pressure, myocardial resistance and blood viscosity may also have an affect on the coronary flow and thereby the CFR[36-38] . Statins have been shown to improve CFR both after long term administration but also in acute phase, only one hour after administration[39-41].

Adenosine is an endogenous substance found in mammals and plays an important role in modulating vascular resistance. There are four G-protein coupled receptors for adenosine: A1, A2A, A2B, and A3. Receptor type A2A and A2B are coupled to a specific subunit of the G-protein which activates Ca^{2+} channels whilst A1 and A3 inhibit Ca^{2+} conductance. In mouse, A2A receptors are responsible for vasodilatation of coronary arteries and A2B in the aorta. There is a higher density of receptors in the

heart than in peripheral vasculature[42, 43]. The mechanism for the adenosine-mediated vasodilatation is not entirely understood, but is most probably mediated through both nitric oxide-independent and nitric oxide-dependent pathways[44].

Ultrasound imaging

Ultrasound is emitted sound that is inaudible for humans. The theory behind ultrasound based imaging is; emitted sound hits a surface and the sound is emitted back to the transducer as an echo and is projected as an image[45]. The ultrasound transducer, or probe, normally consists of piezoelectric crystals that vibrate when an electric current is applied. This creates sound waves that penetrate matter with different depth. The higher the frequency of the probe, the shorter the wave length and consequently a shorter penetration depth in the tissue. The frequency (in Hz) of the transducer is determined from the thickness of the element of the piezoelectric crystal layer. A high-resolution ultrasound thus generates images at a greater resolution but only in tissue closer to the surface from the probe. Frame rate (Hz/s) is also dependent on the probe frequency. Frame rate is the time it takes for the ultrasound to be emitted, reflected and projected as an image. The deeper into the tissue the ultrasound goes the longer time it takes for the echo to be reflected, which means that frame rate is decreased with increased depth. So, what is won in resolution is lost in depth. Another factor affecting the ultrasound images is angle. The ultrasound wave is most accurately reflected when the tissue is at a 90 degree angle to the beam. Otherwise the reflected signal could be underestimated.

The Doppler technique

A variant of the ultrasound technique is a low frequency color Doppler application. The color-guided technique allows detection of movement of objects exposed the ultrasound beam[45]. This can be applied to measure blood flow velocity since the red blood cells are reflecting echo. Blood cells moving toward the transducer will reflect a higher frequency than the emitted, whilst blood cells

moving away from the transducer will send back a lower signal than the emitted. Using Color Doppler echocardiography this technique is applied for measurements of both velocity and direction of the blood flow.

Imaging in atherosclerosis research

The high-frequency ultrasound biomicroscope (UBM) with both a high temporal and spatial resolution, was first developed by Foster et al.[46]. The UBM has then been applied in mice both for embryonic and cardiovascular imaging of central and peripheral artery morphology[47-49]. Recently, a paper was published in carotid plaque imaging in atherosclerotic mice using UBM[50]. Other high-resolution imaging techniques include magnetic resonance imaging (MRI) which has been used for investigation of size and composition of atherosclerotic plaques in mice[51-54]. For investigation of coronary artery function together with morphological measurements of the LCA, Color Doppler echocardiography and UBM was first applied in mice by our group[55-57]. The CDE has also been used for aortic flow velocity measurements in detection of atherosclerosis[58]. For morphological studies of coronary artery atherosclerosis and imaging of myocardial infarction in mice, an invasive micro-angiography technique have previously been applied, both *in vivo*[59] and *ex vivo*[60].

AIMS OF THE THESIS

The overall aim of this thesis was to develop and apply ultrasound-based imaging techniques in morphological and functional studies of atherosclerotic mice.

The specific aims of this thesis were:

- To develop an *in vivo* protocol for investigation of both coronary artery atherosclerosis and function in mice using Color Doppler guided echocardiography
- To develop high-resolution *in vivo* methods to investigate aortic and brachiocephalic atherosclerotic plaques in mice
- To investigate how a known risk factor (interleukin-18) correlates with the development of coronary artery atherosclerosis in mice
- To apply the developed ultrasound techniques in an interventional study using atherosclerotic mice treated with rosuvastatin

METHODS

Animals and diets

The apolipoprotein E knock-out (**ApoE KO**) mouse on a mixed background of 129SvJ and C57BL/6 (Taconic, Denmark) used in paper IV and V, were fed a LARD diet (21% pork lard, 0.15% cholesterol, SDS, Witham, UK). This diet increases the plasma total cholesterol levels (to approximately 40 mM) and thereby accelerates atherosclerosis.

The low density lipoprotein receptor knock-out (**LDLr KO**) mouse on a mixed background of 129SvJ and C57BL/6 (Taconic, Denmark) was used in paper II and fed Western diet (21% milk fat, 0.15% cholesterol, Lactamin) for 30 weeks prior to switching to a standard diet for the final 8 weeks prior to study end. Their plasma total cholesterol levels at the end of the study averaged at 10 mM.

The apolipoprotein E/low density lipoprotein receptor double knock-out (**ApoE/LDLr DKO**) mouse on a mixed background of 129SvJ and C57BL/6 (Taconic, Denmark) on was used as the animal model in paper I and III. These animals were fed a standard chow (5% fat, 0.01% cholesterol, Lactamin) during the entire study. Without the high-fat diet the animals had lower plasma total cholesterol levels (14.4 mM at 10 weeks, 21.6 mM at 40 weeks, and 23.2 mM at 80 weeks of age).

The wild-type mice **C57BL/6** (Charles River Laboratories, Sulzfeld, Germany) were used in papers I, II and III as a non-atherosclerotic control and in paper II for validation of adenosine dose. The wild-type mice fed a standard chow have total cholesterol levels of about 2 mM and do not develop atherosclerosis.

All three of the genetically modified mice used in this thesis develop atherosclerosis to a more or less extent, depending on knock-out model and diet. The atherosclerotic progression starts

in the aortic root and spreads to the ascending aorta and further out to the coronary arteries, neck-vessels and descending aorta and abdominal aorta. The C57BL/6 mice do not develop atherosclerosis when fed a standard diet but have been shown to develop small atherosclerotic lesions in the aortic root when they are fed a high-fat diet for one year[61].

Comments
In this thesis, male mice have been chosen for the in vivo studies. Male mice have shown increased atherosclerotic progression and the male ApoE KO mouse also responds to statin treatment[61, 62].

A short summary of the genetic modifications in these mice: the apolipoprotein E is part of chylomicron remnants that are brought to the liver for clearance. Consequently, this ApoE knock-out mouse model develops hypercholesterolemia-driven atherosclerosis. The low density lipoprotein receptor knock-out (LDLr KO) mouse lacks of the LDL receptor, mainly situated in the hepatocyte membrane[17]. This deficiency leads to decreased clearance of circulating LDL particles containing cholesterol thus increasing hypercholesterolemia-driven atherosclerosis in this model. The ApoE/LDLr DKO mouse lacks both genes which accelerates atherosclerosis without a high-fat diet feeding.

Ultrasound imaging

The preparations for a successful ultrasonic examination are good and light anesthesia to maintain close to physiological conditions and a good contact between the ultrasound probe and mouse using ultrasound gel. During all our ultrasonic experiments the animals were anesthetized with isoflurane gas (Forene isoflurane, Abbott Scandinavia AB, Sweden) and kept sedated with a dose of approximately 1.5% isoflurane in room air, resulting in a heart rate around 400 beats per min. The fur from the anterior chest wall is removed using a chemical hair remover. During the examination the mice were kept on a heated bench and warm ultrasound transmission gel was applied on the chest before scanning.

Ultrasound biomicroscope (UBM)

A UBM system (Vevo 770, Visualsonics, Toronto, Canada) equipped with a 40MHz mechanical transducer was used for all the high-resolution imaging examinations. The maximum penetration depth of this specific transducer is 1.2 cm with a centre focus at 6 mm. The 40MHz scan head has a theoretic resolution of 40 μm and operates with a frame rate of 32 Hz/s.

Ascending aorta

A right parasternal long axis view (LAX) was used to visualize the ascending aorta, aortic arch and the neck vessels in one plane. A short axis view (SAX) is used for capturing cross sectional loops for comparison with histology (figure 1A). A 10 s CINE loop is stored digitally for off-line analysis using the Vevo 770 software (Vevo 770, Visualsonics, Toronto, Canada). At off-line analysis all the images were analyzed blinded to the identities of the animals. Aortic intima media thickness (IMT) was measured at the far ascending aorta wall from the leading echo edge (intima) closest to the blood stream to the next leading echo edge representing the layer of adventitia[47, 63]. In the short axis images, the maximum plaque thickness was averaged from three lesion sites around the thickest part of a plaque, approximately 100 μm apart from each other. Plaque area was delineated by also using the leading-to-leading edge approach, which includes the underlying smooth muscle cell layers in the plaque area measurement.

Brachiocephalic artery (Br)

The brachiocephalic artery is visualized in a LAX and SAX view, from the aortic to the subclavian bifurcation in one plane (figure 1B). In the off-line analysis the largest plaque seen in the stored sequence was chosen for plaque area measurements. A similar protocol as for the aorta was used for the brachiocephalic artery analysis with the exception that smooth muscle cells were not included in the plaque area measurements.

Left coronary artery (LCA)

When imaging the proximal ascending aorta in a short axis view the probe was slightly tilted laterally. In this projection a long axis view of the left coronary artery was visualized (figure 1C). Both the average diameter over the first millimetres of the LCA and the narrowest lumen can be measured in the UBM images of the LCA (see Appendix). The total vessel diameter and outer and inner lumen diameter was measured in diastole, when LCA is maximally dilated.

Comments

The reason for sampling both LAX and SAX images of the aorta and brachiocephalic artery is that the images both complement and confirm each other, which will increase the accuracy of the plaque measurements.

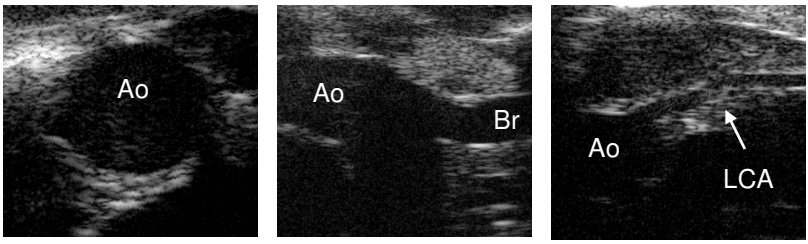

Figure 1. Images from the UBM; A cross-section of the ascending aorta, B long-axis view of the aorta and brachiocephalic artery, C long-axis view of the left coronary artery
(Ao = aorta, Br = brachiocephalic artery, LCA = left coronary artery)

Color Doppler Echocardiography (CDE)

Basic echocardiography

Echocardiography was performed using a high-frequency 15-MHz linear transducer (Entos CL15-7, Philips Medical Systems, Bothell, Washington) connected to an ultrasound system (ATL-HDI5000, Philips Medical Systems). The maximal theoretical resolution of the 15MHz probe is 150 μm and the frame rate is 230 Hz/s. All

cardiac measurements were made in accordance with guidelines from the American Society of Echocardiography[64]. Stroke volume (SV) and the end-diastolic volume (EDV) were calculated using the cubic formula, and ejection fraction (EF), fractional shortening (FS) and cardiac output (CO) were calculated from previously validated formulas[65]. Left ventricular mass (LVM) was calculated according to the area-length formula[66]. All off-line measurements were made using MedArchive viewer 2.1 (Secure Archive, Indianapolis, IN, USA) or Image Arena software (Image Arena 2.9.1, Tomtec Imaging Systems GmbH, Germany).

Assessment of left coronary flow velocity

Doppler flow measurements were made in both the proximal and mid segment of the LCA. The heart was imaged using a parasternal long-axis view with the probe lateralized and the ultrasound beam anteriorly tilted. In this image window, the entire LCA, from the aortic sinus to the distal branch site, could be visualized using CDE. The course of the LCA was typically parallel to the Doppler beam, which also facilitates Doppler measurements without any angle correction. A 6-MHz pulsed Doppler with a gate size of 0.5 to 1 mm was used. Mean diastolic flow velocity was obtained by outlining the diastolic phase of coronary flow signals in an off-line software program (MedArchive, Secure Archive, Indianapolis, IN, USA or Image Arena 2.9.1, Tomtec Imaging Systems GmbH, Germany). Measurements were averaged from three consecutive cardiac cycles.

Velocity ratio

For the velocity ratio (Vratio) assessment a value from both the proximal part and mid part from the LCA was obtained. The Vratio was calculated as the proximal flow velocity divided with the mid flow velocity. Atherosclerotic mice seem to develop proximal coronary artery atherosclerosis unlike humans were the atherosclerosis is more distally localized[67]. This means that mice with coronary artery stenosis will have enhanced flow velocity values in the proximal part compared with the mid part, and thus an increased Vratio.

Coronary artery function

In the CFVR protocol the flow velocity measurements were made at the same vessel site (either at proximal or mid site) during baseline and hypoxia or adenosine-induced hyperemia. The CFVR was thereafter calculated as the mean diastolic flow velocity during hyperemia divided by the baseline. In the interventional study (paper V) we chose to look at the volumetric flow at baseline and hyperemia separately instead of the reserve. Flow is calculated by measuring LCA-segment length and area, assessed by the UBM, combined with the velocity time integral values measured with CDE (figure 2). The UBM-measurements were made in diastole, when LCA is maximally dilated.

Adenosine

Doppler measurements were made at baseline and during adenosine-induced hyperemia (paper II, V). Infusion of 140-160 μg/kg/min of adenosine were facilitated via the tail vein as described above. This dose was validated to induce coronary hyperemia without influencing systemic hemodynamics, as validated in C57BL/6 mice (paper II). This dose seems to induce maximum coronary hyperemia, because an additional dose of 320 μg/kg/min in C57BL/6 mice did not further increase the hyperemic flow velocity. Maximal hyperemia was typically obtained within 2 to 3 min.

Hypoxia

Flow velocity measurements were made at baseline and during hypoxia-induced hyperemia for a maximum of 3 min (paper II). Moderate hypoxia was induced during anesthesia by changing the mixture of air and nitrogen gas into the gas mask. Baseline oxygen tension was 21% in air with no addition of nitrogen gas. Hypoxic gas mixture with an oxygen tension of 12.5% was obtained by quick reduction of air and addition of nitrogen gas.

Comments

The use of volumetric flow (μl/min) in the LCA during baseline and adenosine-induced hyperemia was used in paper V instead of the CFVR. We showed recently that coronary artery diameter in

both wild-type and ApoE KO mice increased following adenosine infusion, which may imply that CFVR might slightly underestimate the true coronary flow[68]. In paper V we wanted to investigate the potential treatment effects in baseline and hyperemia separately.

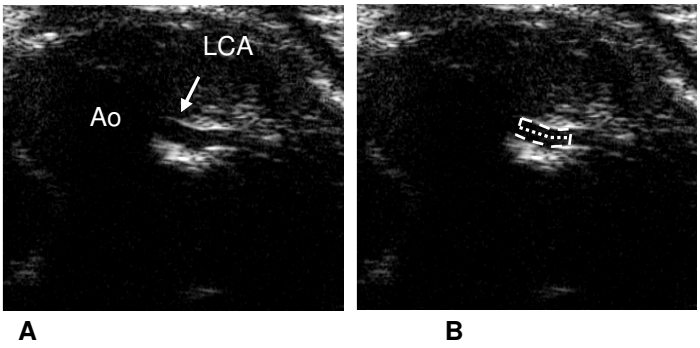

Figure 2. A. UBM visualization of the proximal LCA, B. with measurements of LCA area and LCA area segment length.

Lipid extraction

Frozen liver tissues were homogenized in methanol, and the protein concentration was measured according to standard protocol[69]. Liver lipid extraction was performed with methanol and chloroform[70]. A normal-phase HPLC system was used for lipid class separation according to Homan et al., with slight modifications[71]. Lipid classes were detected using an evaporative light scattering detector (PL-ELS 1000, Polymer Laboratories, Amherst, MA, USA). Calibration curves for detector response versus mass of lipid were obtained by injecting lipid standards. The results are presented as mass of lipid corrected for amount of protein recovered.

Comments
This technique will in the future be applied to study mechanisms underlying lipid lowering effects of treatment. In this study (paper V) it was used to analyze whether the statin treated mice suffered

from liver steatosis, which was not the case apparently in either of the groups.

Histology and immunohistochemistry

As a standard procedure at study end in this thesis the heart, aorta, and brachiocephalic arteries were dissected out after a quick rinse with saline solution and fixed in formaldehyde before being embedded in paraffin. Serial cross sections of 5μm were made using a microtome (RM2255, Leica Microsystems) form the ascending aorta, at different sites on the brachiocephalic artery (proximal and mid-brachiocephalic and more distally at the bifurcation with the subclavian artery) and the proximal part of the heart and coronary arteries (from the aortic sinus to the mitral valve). The sections were placed on TechMate slides (ChemMateTM Capillary Gap Microscope Slide S2024, DakoCytomation).

For cross-sectional plaque area measurements and collagen content quantification, sections were stained with Picro Sirius Red (Histocenter, Gothenburg, Sweden). For macrophage accumulation, sections were stained with a Mac-2 antibody at a dilution of 1:15,000 (CL8942AP clone M3/38, Cedarlane). Quantitative measurements of collagen and macrophage content as percentage of plaque area were made using Image-Pro Plus 5.1.2 software (MediaCybernetics, Bethesda, MD, USA).

For qualitative localization of IL-18 protein in atherosclerotic plaques, rabbit anti-human antibody (ProteinTech Group Inc, Chicago, IL, USA) at a concentration of 1:500 was applied to tissue sections. All the immunohistochemical staining procedures were automated using TechMate 500 (DakoCytomation, Glostrup, Denmark). Prior to the immunohistochemical analysis, the antibodies were pre-incubated with the corresponding protein to confirm the specificity.

Plasma analysis

Blood samples were collected from the saphenous vein during the studies and obtained via heart puncture under 1.5% isoflurane anesthesia (Forene isoflurane, Abbott Scandinavia AB, Sweden) at study end. Samples were placed in lithium heparin-containing tubes, centrifuged at 4ºC and 2000 x g for 10 minutes. The plasma was then stored at -80ºC until analysis of total cholesterol, IL-18 or SAA. Total cholesterol levels were analyzed using commercial reagents (cat. no. 12016630, Roche Diagnostics, GmbH, Mannheim, Germany) and Cobas Mira Plus (Roche Diagnostics) with enzymatic-spectrophotometric methods. The levels of the acute inflammatory parameter serum amyloid A (SAA) were analyzed using a Murine Serum Amyloid Enzyme Immunoassay kit (cat. no. TP802-M, Tridelta Development LTD, Ireland). IL-18 levels in the plasma were measured by following the manufacturer's protocol for the ELISA kit (R&D Systems Inc., Minneapolis, MN, USA).

Statistics

Data in all papers are presented as mean ± standard error of mean (SEM) with the exception for paper II where data are presented as mean ± standard deviation (SD). A p value <0.05 was considered statistically significant except when a Bonferroni correction was used. For correlation testing between two parameters, Pearson´s linear regression test (paper II-V) or Spearman non-parametric correlation test (paper I) were used. Differences between two parameters at a certain time point were tested by using Student's t test with a Bonferroni correction for multiple comparisons (paper II and V). When time-dependent change where compared, one-way analysis of variance (one-way-ANOVA) with Bonferroni post hoc test was used, once the ANOVA showed significance. Repeated measurement 2-way ANOVA was used together with Student's t test in each time point, only when the 2-way ANOVA tests showed significance. For methodological validation and comparison of UBM and histology-assessed measurements of

plaque area, Bland-Altman analysis was used to show individual variations compared to the average values from both of the methods. The coefficient of variation for inter-observer variability was calculated using the following formula: standard deviation (x-y)/mean (x,y) x 100. All statistical analysis was performed using Prism 4.0 (Graphpad Inc., San Diego, California).

Comments

With the exception of paper I, we chose to statistically analyze our data as parametric. The data in the particular study show similar correlations independently of parametric or non-parametric correlation analysis.

SUMMARY OF RESULTS

Methodological validations (paper I-III)

Coronary artery atherosclerosis can be assessed non-invasively in mice using ultrasound imaging (paper I)

In paper I we established a new technique to investigate coronary artery atherosclerosis *in vivo* in a non-invasive manner in mice. Using color Doppler guided echocardiography in ApoE/LDLr DKO mice we measured flow velocity in both the proximal and mid part of the left coronary artery (figure 3). The ratio between these two sites is the velocity ratio (Vratio). To confirm the Vratio data we measured the degree of LCA atherosclerosis using both the recently developed UBM-technique and histology.

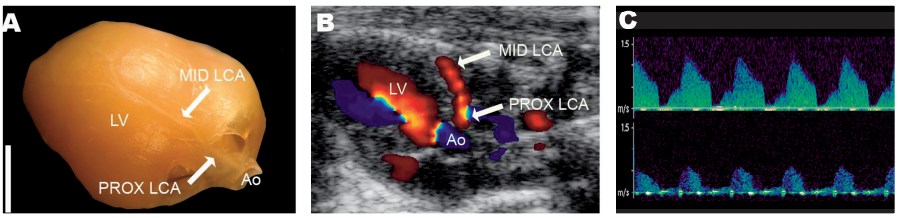

Figure 3. The figure illustrates a formalin-fixed mouse heart with the left coronary artery (A) and its corresponding image visualized with color Doppler echocardiography (CDE) (B). Figure C, is showing the CDE-assessed flow velocity in the proximal part of LCA in an atherosclerotic mouse (upper profile) and in the mid part (lower profile).

The results from the first paper show that Vratio increase with age in 10, 40 and 80 weeks old ApoE/LDLr DKO mice (P=0.0055). Vratio correlates to percentage wall thickness in the left coronary artery (LCA), measured both by ultrasound biomicroscope (P=0.0044, r=0.65) and histology (P=0.0002, r=0.78, figure 4).

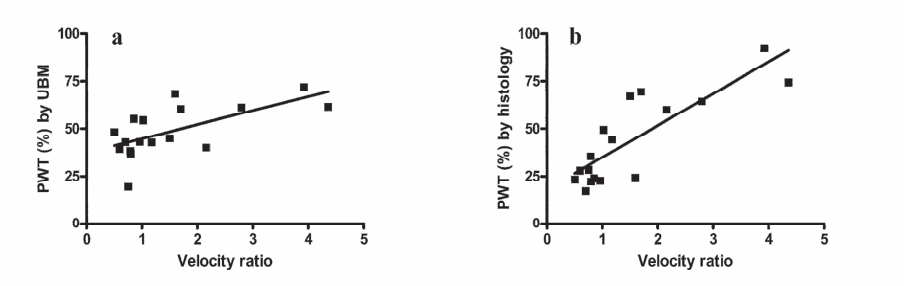

Figure 4. Graph showing the correlation between velocity ratio and percentage wall thickness assessed with (a) UBM (P=0.0044, r=0.65) and (b) histology (P=0.0002, r=0.78)

This technique provides us with a quantitative tool to assess coronary artery atherosclerosis in mice in real-time with a resolution down to 40 μm. Contrary to the more distal part of the LCA, the proximal portion of LCA, which is epicardially localized, can be easily visualized both with color Doppler and UBM. Mice develop proximal rather then distally located atherosclerotic lesions in the coronary arteries compared to humans[67]. This seems to be the reason for increased flow velocity in the proximal part rather than mid part in atherosclerotic mice (figure 5).

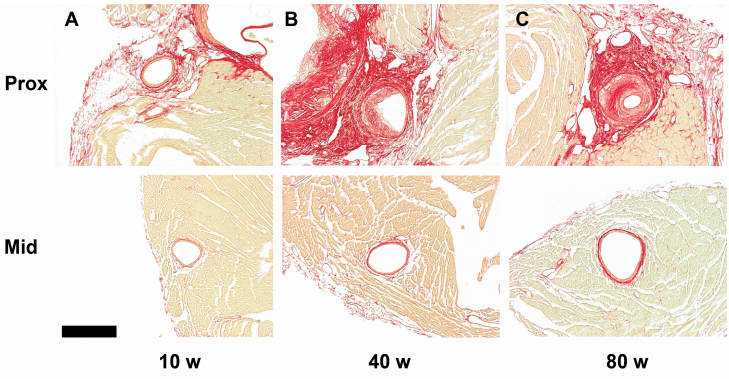

Figure 5. Illustration of histological images of the LCA. Upper panel represents the proximal LCA in A. 10 weeks old, B. 40 weeks old and C. in 80 weeks old ApoE/LDLr DKO mice. Lower panel represents the corresponding images from the mid LCA.

In conclusion, coronary artery atherosclerosis can be measured in vivo and non-invasively in mice using color Doppler echocardiography.

Ultrasound-based coronary flow velocity reserve can be assessed in living mice (paper II)

In paper II we investigated the ability to use the coronary flow velocity reserve (CFVR) approach in atherosclerotic LDLr KO mice and in wild type C57BL/6 mice. Using color Doppler echocardiography and either hypoxia or adenosine in anaesthetized mice, we achieved maximal hyperemic flow velocity. CFVR is the ratio between the hyperemic flow velocity and the basal flow velocity (figure 6). UBM was used for assessment of minimal lumen diameter of the proximal left coronary artery.

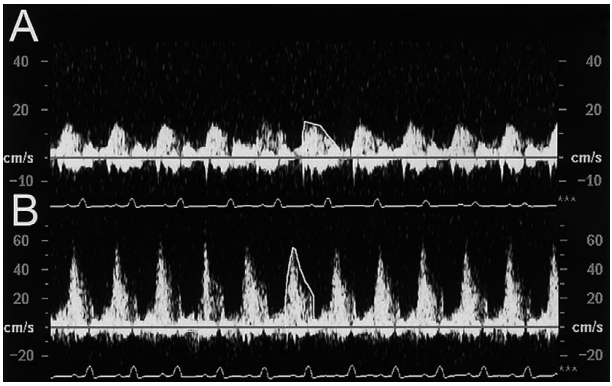

Figure 6. Diastolic basal flow velocity (delineated) in the mid part of the LCA (A) compared to the hyperemic flow velocity (B).

This study reveals that CFVR can be induced in mice using either hypoxia or adenosine. The results also show that hypoxia-induced CFVR correlates with UBM-assessed minimal lumen diameter ($P<0.005$, $R2=0.8707$, figure 7) in the LDLr KO mice. The presence of proximal lumen narrowing was confirmed with histological sections of the LCA. In addition, this paper also includes a validation study in C57BL/6 mice. We investigated which dose of adenosine to use without receiving circulatory effects such as decreased blood pressure or changes in heart rate. These results show that a dose of 160 μg/kg/min caused maximal hyperemia without affecting blood pressure.

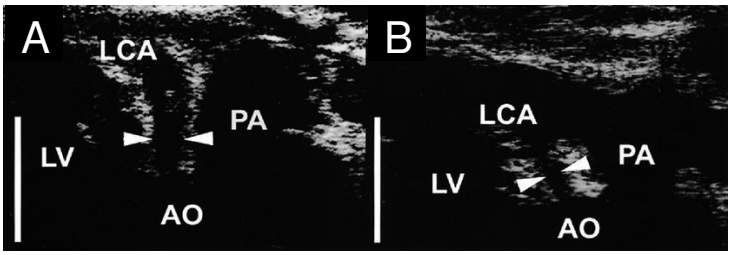

Figure 7. UBM-assessed images of LCA in (A) a non-atherosclerotic wild-type mouse compared to an atherosclerotic LDLr KO mouse (B). Arrows indicate the minimal lumen diameter. Scale bar = 1mm.

In conclusion, coronary flow velocity reserve can be assessed in mice using either hypoxia or adenosine. The CFVR correlated with minimal lumen diameter of LCA in this animal model of atherosclerosis.

Atherosclerotic lesions in mice can be assessed *in vivo* using high-resolution ultrasound biomicroscopy (paper III)

In paper III, we investigated the ability to use UBM for quantitative imaging of aortic atherosclerotic plaques in living atherosclerotic ApoE/LDLr DKO mice at ages 10, 34, 40 and 80 weeks. Using the UBM with the 40 MHz probe we obtain a spatial resolution down to 40 μm and were thus able to measure atherosclerotic lesions (figure 8).

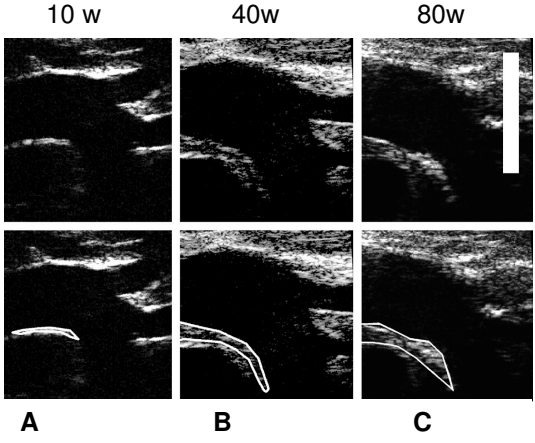

Figure 8. The upper panel illustrates a long axis view of the aortic arch in 10, 40 and 80 weeks old ApoE/LDLr DKO mice (A, B and C respectively). In the lower panel the atherosclerotic lesions are delineated. Scale bar = 2 mm.

The plaque thickness assessed from histology significantly correlated with ultrasound-measured intima media thickness (IMT) in SAX view ($p < 0.0001$, Pearson $r = 0.91$, figure 9a). The results also reveal that histological assessed plaque area correlated significantly with UBM-measured plaque area in the SAX view ($p < 0.0001$, Pearson $r = 0.94$, respectively, figure 9b).

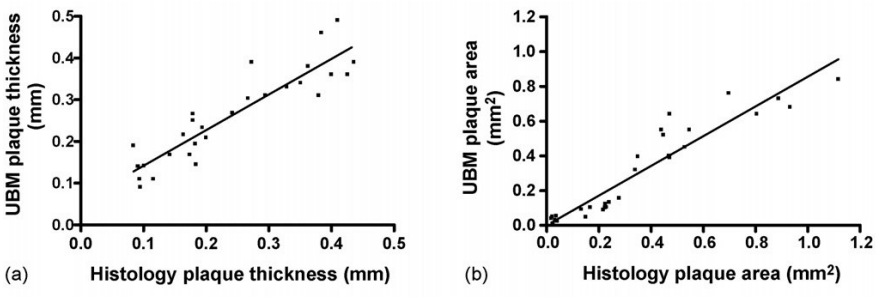

Figure 9. (a) Correlation between UBM and histology-assessed plaque thickness; (b) Significant correlation between UBM and histology-assessed plaque area in the cross-sectional views of the ascending aorta.

In a separate study in this paper we used mice at ages 32, 33, 34 and 35 weeks old to test the accuracy of UBM to distinguish between the IMT in mice closer in age ($P=0.0002$). We found that UBM was able to distinguish the differences in IMT in the aorta of these animals close in age. Also, since a good correlation was found between histology and UBM plaque area during both systole and diastole in both LAX and SAX views, we chose to use the diastolic values in the future, since it may better reflect the pressure-less situation in the *ex vivo* histological preparation. Using Bland-Altman analysis the difference between UBM and histologically assessed plaque thickness was relatively uniform and did not seem to increase with increased plaque thickness. Compared to histology, UBM seems to overestimate the IMT and systematically underestimate the histologically assessed plaque area values.

In conclusion, UBM is a highly feasible and non-invasive technique, which allows accurate real-time imaging of atherosclerosis in mice aorta. Using IMT measurement, progression of atherosclerosis can be followed on a weekly basis in ApoE/LDLr DKO mice.

Methodological applications (paper IV-V)

Coronary artery atherosclerosis correlates with circulating IL-18 expression in ApoE KO mice (paper IV)

In paper IV we wanted to investigate the potential relationship between coronary artery atherosclerosis using our velocity ratio protocol (from paper I) and circulatory IL-18. IL-18 is a cytokine found to be present in atherosclerotic plaques and elevated in serum in patients with coronary artery disease[10, 11]. The findings in paper IV reveal that velocity ratio correlates with the circulating level of IL-18 implying that increased atherosclerosis in the LCA is associated with enhanced levels of plasma IL-18 ($P<0.01$, $r=0.75$, figure 10A). The IL-18 levels also correlate with the percentage of macrophages present in the aortic plaques ($P<0.001$, $r=0.91$, figure 10B). Histological sections stained for IL-18 showed that IL-18 seems to be present in macrophages in the plaques.

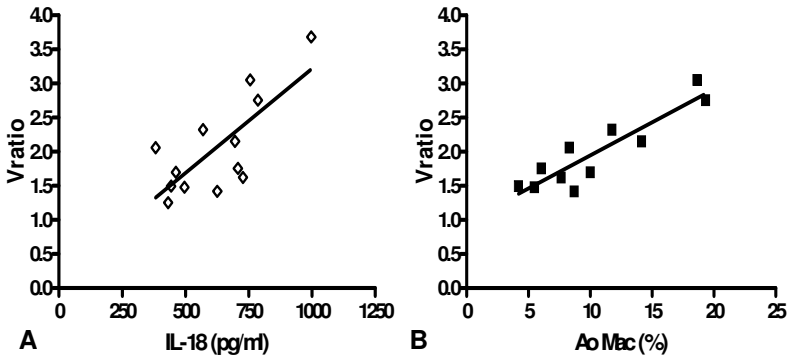

Figure 10. A. Correlation between Vratio and circulating IL-18 levels after 15 weeks of diet ($p<0.01$, $r=0.75$). B. The percentage of macrophages in aortic plaques compared to Vratio ($p<0.001$, $r=0.91$).

In conclusion, the results from paper IV suggest that IL-18 plays a role in the development of coronary artery stenosis in this advanced mouse model of atherosclerosis.

Ultrasound-based imaging can be used for detection of cardiovascular effects following statin treatment in mice (paper V)

In paper V we treated ApoE KO mice with LARD diet with or without rosuvastatin for 16 weeks. Every fourth week blood samples were collected for total cholesterol measurements and high-resolution UBM technique was applied for investigation of the plaque progression during the interventional study. The results revealed a decrease in plasma total cholesterol in the rosuvastatin treated group starting after four and remaining until 16 weeks of treatment (2-way ANOVA, $P<0.05$, figure 11).

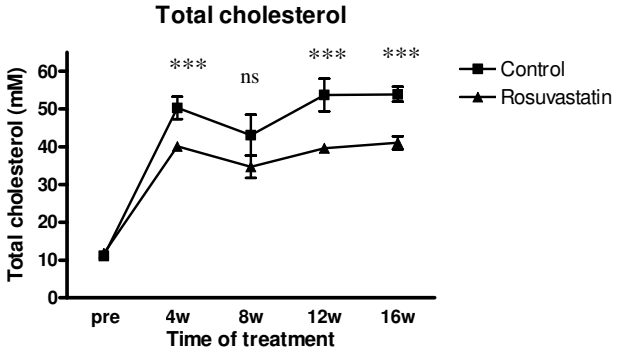

Figure 11. Plasma total cholesterol levels in controls and rosuvastatin treated mice before treatment onset and after 4, 8, 12, and 16 weeks.

This was accompanied by retardation in brachiocephalic artery lesion progression in the treated group as shown in LAX and SAX views with UBM (2-way ANOVA, $P<0.001$ and $P<0.05$ respectively, figure 12) and at study end by histology ($P<0.05$).

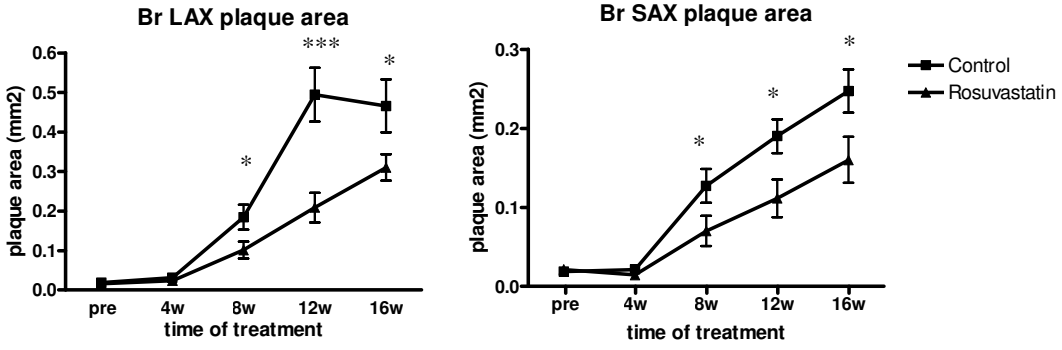

Figure 12. UBM-assessed plaque area progression in the brachiocephalic artery over time of treatment in two different projections; to the left a long-axis view (LAX) and to the right in a short-axis view (SAX).

At the end of the study the coronary volumetric flow was measured in baseline and hyperemia using the vasodilating substance adenosine. Flow was increased during adenosine infusion in the treated group compared to controls (P<0.001, figure 13). Also the plasma marker for inflammation serum amyloid A (SAA) was reduced in the treated group (P<0.001).

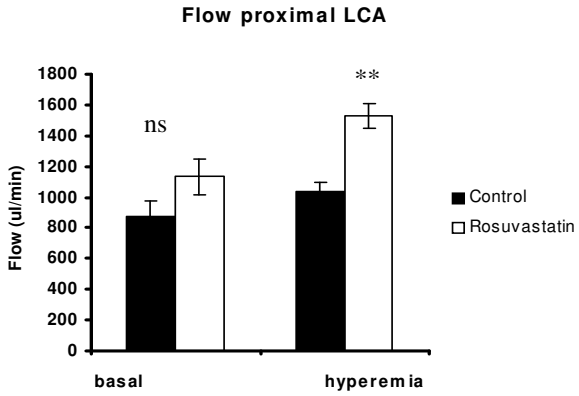

Figure 13. Volumetric flow at study end during baseline and adenosine-infusion in controls compared to treated mice.

In conclusion, effects of treatment on atherosclerotic lesion progression can be followed on a regular basis using UBM. All our findings from this study suggest an improved cardiovascular status using rosuvastatin in male ApoE KO mice. This animal model fed a LARD diet and treated with rosuvastatin thereby provides us with a robust animal model with a statin-responding phenotype, which may facilitate future translational drug intervention studies in mice.

DISCUSSION

Ultrasound-based imaging of atherosclerotic lesions in mice

Using the high-resolution ultrasound technique we found a good correlation between UBM and histology-assessed plaque area and plaque thickness in the aorta and plaque area in the brachiocephalic artery. However, due to differences between the *in vivo* and *ex vivo* situation, such as the cardiac cycle, blood pressure and *ex vivo* histological shrinkage, caution should be taken for accurate measurement. Thus, we present in paper III and V the validated protocols for optimal plaque measurements in aortic and brachiocephalic arteries, respectively.

Ultrasound biomicroscopy has gained increased usage in recent years mostly within mouse embryonic research[72]. With a resolution down to 40 μm and a frame rate of 32 Hz, UBM is theoretically suitable for *in vivo* study of the murine cardiovascular systems. Recently, Zhou et al. showed that several major peripheral vascular systems could be imaged using UBM in adult mice[48]. However, the accuracy and feasibility of the technique to assess atherosclerotic lesions in adult mice have not previously been validated. The 40MHz scan head used in all papers of this thesis has a fixed focus depth at 6 mm, which may in some cases complicate the imaging windows and require skilled operators to obtain good image quality. However, with training, the feasibility is extremely high and the technique is well tolerated by the animals, due to the short scanning and anesthesia time. Average time needed for scanning is below 8 min per mouse. Also, as shown in paper III, acceptable intra- and inter-observer variability can be achieved regarding measurement of both intima-media-thickness (IMT) and lesion area. The progression of atherosclerosis can even be followed on a weekly basis using IMT measurement.

Three-dimensional fast spin-echo magnetic resonance imaging has been used to image atherosclerosis in mouse innominate arteries with a typical resolution of 140 μm isotropic resolution[51]. The

procedure takes approximately 30 min. Using implanted coil a resolution of 25 μm can be obtained[73]. However, the latter technique is invasive and the procedure is much more complicated than the one described by Hockings et al. Thus, UBM is a highly feasible, non-invasive and uncomplicated technique, which allows accurate real-time imaging of atherosclerosis in all the major peripheral vascular systems in mice.

Morphological and functional imaging of coronary arteries in mice

Flow velocity measurements using CDE

Prior to this work, we developed a technique to assess mouse coronary artery flow velocity *in vivo* with great success rate and good reproducibility using transthoracic color Doppler echocardiography[74]. In mice with small vascular structures and extremely high heart rate, there are so far no established non-invasive methods for quantification of mouse coronary artery function and morphology.

CFVR method

In paper II we further developed this imaging procedure, where we assessed the CFVR protocol to investigate mouse coronary artery function. CFVR or its volumetric counterpart CFR is induced by infusion of vasodilating substances. The two techniques are used clinically to address hemodynamic relevance of stenosis[75, 76]and for investigation of myocardial microvessel status[32, 77, 78]. Adenosine is commonly used in clinical practice to induce the maximum coronary hyperemia. In paper II we showed that similar hyperemic values are achieved using either adenosine or hypoxia in wild-type C57BL/6 mice. Using the protocol in the LDLr KO, the results also reveal a good correlation between hypoxia-induced CFVR and minimal lumen diameter (MLD). This indicates a lowering in ability to raise flow at increased oxygen demand when the vessel lumen is narrowed by atherosclerosis in this animal model. CFVR has been used previously to predict coronary stenosis and MLD in atherosclerotic coronary arteries in man[34, 75].

In a general population of patients with coronary artery disease and multiple cardiovascular risk factors, a CFVR value <2.0 has been shown to comprise high sensitivity and specificity for prediction of hemodynamically significant coronary artery stenosis irrespective of other risk factors[75]. In mice hearts, *ex vivo* perfusion studies have shown that adenosine usually induces resistance lowering and a flow increase that correspond to a CFR between 1.4 and 4.4[42, 79-81]. Our results from paper II show that the average CFVR values from both the C57BL/6 mice and the LDLr KO mice are <2. The differences in flow responses reported in the above mentioned studies and our studies, are most probably attributable to differences in adenosine concentrations and other methodological differences, such as basal metabolism and oxygen saturation of the perfusion medium. Also, the CFVR values induced in mice in our study averaged at 2, whereas corresponding values in healthy humans usually exceed 3. This discrepancy may be explained by several factors. First, the housing of mice in cages without voluntary daily physical activity may result in reduced cardiac performance. Second, one may speculate that the small body size and the high HR could lead to an elevated basal metabolism with corresponding lower cardiac reserve capacity compared with humans. Third, it is also now evident that mice are only capable of increasing their oxygen uptake by a factor of two when they are forced to run on a treadmill[82], compared with the nearly 20-fold increase in humans.

Velocity ratio

With time atherosclerotic lesions tend to become lumen-obstructive. Lumen-narrowing plaque growth is associated with locally increased flow velocity, a hemodynamic phenomenon, which is widely used in, for example measurement of carotid artery stenosis[83]. The velocity ratio between prestenotic and stenotic flow in the left coronary artery using CDE has previously been applied to determine the degree of restenosis in patients undergoing angioplasty[84, 85]. Mouse coronary artery stenosis was studied recently by several groups using micro-angiography[59, 60]. However, due to its invasive nature, the technique does not permit repeated measurement in mice. We show in paper I that mouse coronary

artery stenosis can be accurately assessed by using a non-invasive approach. By measuring the proximal and mid LCA flow velocity with CDE we can calculate the velocity ratio which indicates the degree of atherosclerosis of the LCA.

Morphology, percentage wall thickness and coronary artery diameter

In addition to flow velocity measurements and its applications in the CFVR and Vratio protocols we have developed techniques to assess left coronary artery morphology. Contrary to the more distal part of the LCA, the proximal portion of LCA, which is epicardially localized, can be visualized using the UBM imaging windows validated by us. We show in paper I that UBM-assessed wall thickness reflects proximal coronary artery plaque area measured with histology. Left coronary artery lumen diameter can also be measured in a similar manner. This is useful when assessing minimal lumen diameter in atherosclerotic mice, shown in paper II, as well as for diameter change during adenosine infusion, shown in paper V[68]. This technique provides us with a quantitative tool to assess coronary artery morphology in mice in real-time with a resolution down to 40 μm.

Quantification of coronary artery status

To summarize, the advantage with the CFVR protocol and the Vratio is that they complement each other for studies of the coronary arteries. CFVR can be used for microvessel function both in normal and atherosclerotic mice whilst the Vratio is limited to use in stenotic mice. Since the atherosclerotic progression differs over time from early to late phase, we find that it is important to have available methods for investigation of the entire process. In the early phase, before the development of flow-limiting or rupture-prone atherosclerotic plaques, it is important to have methods to study microvessel function of the heart. In the later phase when the vessel wall is affected by severe atherosclerosis the Vratio is favourable. Still, the cut-off values for CFVR and Vratio in terms of detecting flow-limiting stenosis have to be established in mice.

In our experience, the baseline coronary flow differs substantially between different strains. Strain-related difference in coronary artery diameter, myocardial oxygen demand, body temperature, as well as influence of anesthesia might be responsible for the baseline coronary flow differences. The precise underlying mechanism is still under investigation. However, the strain dependent baseline velocities may have minor importance when calculating degree of coronary artery stenosis using the Vratio. The combination of direct morphological imaging and velocity-based measurement assures robust assessment of coronary artery function and atherosclerosis.

IL-18 and coronary artery atherosclerosis

In paper IV we investigated the potential relationship between coronary atherosclerosis evaluated with ultrasound and a known risk factor, IL-18. We detected a positive correlation between IL-18 levels, left coronary atherosclerosis and aortic macrophage content in this study. Analysis of histological sections from both the aorta and left coronary artery revealed local presence of IL-18 protein mainly in macrophages and to some extent also in smooth muscle cells. This has been confirmed previously where IL-18 and its receptor have been found present in vascular endothelial cells, smooth muscle cells and macrophages of human atheromas[10]. Since macrophages produce most of the cytokines that promote inflammation[7], we speculate that the increased macrophage accumulation might contribute to increased IL-18 production. Increased IL-18 levels might then accelerate coronary artery atherosclerosis. High cholesterol levels are thought to precipitate atherosclerosis. Surprisingly, we found no correlation between total cholesterol levels and coronary artery atherosclerosis in our model system. Our data suggest that early and late atherogenesis could be under influence of different cellular mechanisms. While cholesterol levels contribute to the total atherosclerosis burden, the inflammatory drive may aggravate the severity of the atherosclerotic disease during the late stages.

Evidence in the literature points to a causative role for the cytokine IL-18 in promoting the advancement of atherosclerosis. IL-18 has been shown to increase atherosclerotic lesions after exogenous administration in ApoE KO mice, whilst decreasing plaque development in atherosclerotic mice deficient in the IL-18 gene[12, 13]. This specific cytokine has been found in various diseased tissues in mice including liver, spleen, lung and intestines[86]. While IL-18 is not detected in early subclinical atherosclerosis in humans, a recent clinical study showed that IL-18 was an independent predictor of severity of coronary artery atherosclerosis[11].

To summarize the results from paper IV, our data indicate that IL-18 levels increase in mice with advanced atherosclerosis. IL-18 levels correlated positively with the advancement of coronary artery atherosclerosis as well as peripheral artery plaque composition. Though these relationships do not necessarily suggest any causality, our findings may suggest an important role of IL-18 in late stage atherosclerosis in our mouse model. Our findings add to and support the previous findings in mouse models and in humans.

Effects of rosuvastatin in a mouse model of atherosclerosis

Contradictory results have been reported regarding the response of genetically modified mice to statin treatment. In paper V we showed that ApoE KO mice treated with rosuvastatin for 16 weeks had reduced plasma total cholesterol levels and reduced brachiocephalic artery atherosclerotic lesion progression. Beneficial cardiovascular effects similar to ours have been observed in ApoE KO mice on a high-cholesterol diet treated with rosuvastatin; these studies showed both a plasma lipid lowering effect and reduced lesion formation after 12 weeks of treatment[87, 88]. Simvastatin, on the other hand, showed no positive effect in ApoE KO mice after three months of treatment, but lowered total cholesterol levels and reduced atherosclerotic lesions in low-density lipoprotein receptor knockout mice (LDLr KO)[88, 89]. Atorvastatin, developed after simvastatin, has shown positive effects on atherosclerotic lesion progression and cholesterol levels in female ApoE3*Leiden mice[90,

[91]. Further, there are studies demonstrating atherosclerotic plaque reduction and anti-inflammatory effects of rosuvastatin that are independent of its lipid-lowering effect[92, 93].

One explanation for these differences might be related to the physical properties of the different statins. In clinical trials, Rosuvastatin has been shown to be the most potent third generation statin. Statins not only inhibit cholesterol biosynthesis in the liver but also upregulate the expression of low density lipoprotein (LDL) receptors in the liver and thereby enhance clearance of cholesterol-containing LDL-particles from the circulation to the liver[18]. Other possible causes for the inconsistent results of statins in mouse models might depend on the different genetic backgrounds of the knockout mice, the lipid type and cholesterol content of their diet, the site of investigation in the vascular bed, and the gender of the mice. Zadelaar et al. recently published a review describing the most commonly used mouse models in atherosclerotic research and the response of the models to different pharmaceutical treatments[94]. The review states that there is no consensus about which mouse models respond to statins, and that atherosclerotic development can be diminished independent of cholesterol-lowering effects. In paper V, we show that the total cholesterol levels over time correlates significantly with the plaque burden in the brachiocephalic artery as measured by histology. This provides evidence that the plaque regression seen in our study is dependent on the cholesterol-lowering effect from rosuvastatin treatment rather than being a result of another effect of the medication, although additional effects that are independent of cholesterol lowering cannot be ruled out.

Rosuvastatin-treated mice had greater hyperemic flow in the LCA following adenosine infusion compared to control mice. This indicates an improved microcirculatory function after rosuvastatin treatment in these mice. Our data partially concur with previous studies showing improved *ex vivo* artery function in the heart and aortas of ApoE KO mice treated with rosuvastatin, despite unchanged cholesterol levels in these mice. Similar observations have been made in human trials in which both short- and

moderate long-term statin therapy improved coronary flow and coronary flow velocity reserve (CFR)[39-41]. The mechanism underlying improved vessel function seems to be enhanced nitric oxide release from endothelial cells following statin treatment, which has been shown in both cell-based and animal studies. Interestingly, improved coronary function is observed in humans after only one hour of statin infusion[41]. This demonstrates that statins have an effect on microvasculature independent of a cholesterol-lowering effect, which could not occur during that time frame (1 hour). Thus, both coronary flow and CFR could be useful as integrated physiological markers for coronary artery disease since they reflect several of the major risk factors for atherosclerosis (inflammation, endothelial function, microvascular function, and blood viscosity).

In paper IV and V we fed the mice with a LARD diet. This specific diet has been shown to increase the extent of rupture prone lesions in the brachiocephalic artery[95]. The LARD diet induces extensive atherosclerosis in a shorter period of time, especially in this ApoE KO model. Additionally, the male ApoE KO mouse on this mixed background fed a LARD diet has been shown by others to respond to statin-treatment[62].

To summarize, the male ApoE KO mouse treated with rosuvastatin provides us with a robust animal model with a statin-responding phenotype, which may facilitate future translational drug intervention studies in mice.

CONCLUSIONS

In this thesis, we have developed and applied a number of non-invasive ultrasound-based imaging techniques in mouse models for investigation of various relevant aspects of atherosclerotic cardiovascular disease (summarized in figure below). We have established techniques to study coronary artery status using the CFVR and coronary flow protocol in both early and advanced stages of atherosclerosis in mice. In mice with advanced atherosclerosis, we showed that both coronary and peripheral artery plaque size could be measured *in vivo*, as well as coronary artery stenosis using Vratio approach. Further, we showed for the first time that IL-18, a well-validated atherosclerosis risk factor in man, closely correlated to coronary artery disease status in our mouse model of atherosclerosis. Finally we established a mouse model responding to statin treatment, in which our developed ultrasound-based methods were applied.

The established translational functional and morphological imaging platform in combination with our human-like statin-responding mouse model, provide us with powerful tools for future atherosclerosis research.

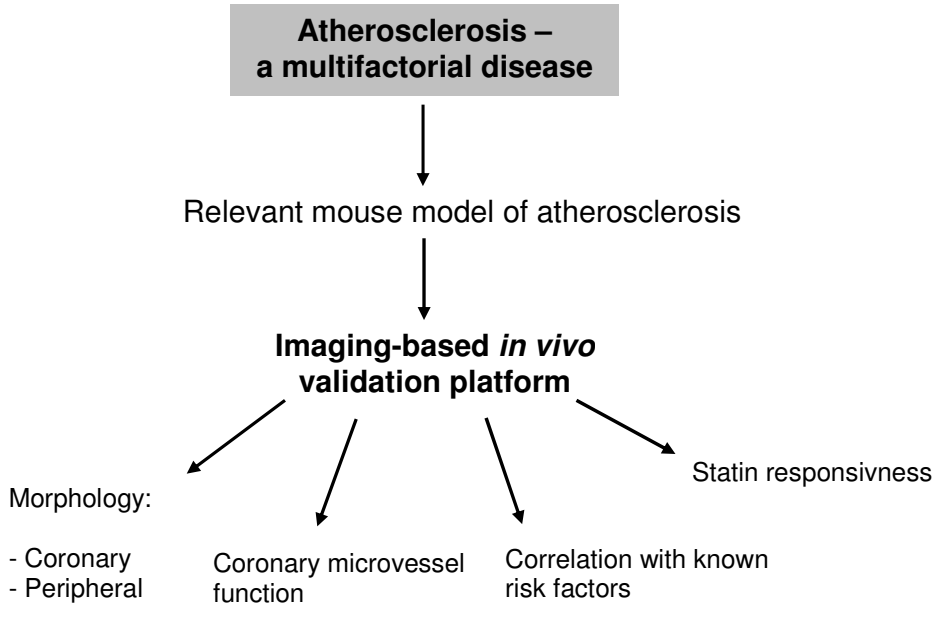

POPULÄRVETENSKAPLIG SAMMANFATTNING

Åderförkalkning är en kalcifierad fettinlagring i blodkärlens vägg och är ofta den underliggande orsaken till hjärtkärlsjukdom. Ett flertal riskfaktorer är associerade med sjukdomen, exempelvis rökning, höga kolesterolvärden, högt blodtryck, fetma och diabetes. Hjärtkärlsjukdom är den vanligaste dödsorsaken i Sverige och i större delar av den industrialiserade världen, vilket medför att forskning inom detta område är väldigt relevant. I nuläget uppnås den bästa forskningen genom att kombinera studier på människa med djur- och cellförsök. Genetiskt modifierade möss som relativt snabbt utvecklar åderförkalkning har öppnat nya vägar för forskarna att studera sjukdomen, som annars har ett långsamt förlopp i människa. Hittills har det inte funnits tillräckligt bra musmodeller som liknar den mänskliga sjukdomsbilden och inte heller tillräckligt bra tekniker för att undersöka sjukdomens utveckling i möss. I denna avhandling har vi utvecklat och tillämpat ultraljudsbaserade metoder för forskning kring hjärtkärlsjukdom i möss.Teknikerna förser forskningsfältet med en bredd för att relevant kunna följa förloppet från tidigt till sent stadie av sjukdomen. Resultaten visar att funktionen i kranskärlen men också storleken på de åderförkalkade placken i både kranskärlen och i kroppspulsådern och halskärl, kan studeras med hjälp av ultraljud. Ultraljudsmetoder möjliggör även att varje mus kan följas på individuell nivå vid upprepade tillfällen. Ett individbaserat undersökningssätt liknar inte bara det sätt man studerar människor på utan möjliggör också att antalet försöksdjur kan reduceras. I avhandlingen finns en behandlingsstudie där en musmodell som utvecklar åderförkalkning behandlats med blodfettssänkande statin. Med hjälp av de utvecklade ultraljudsteknikerna kunde ett flertal fördelaktiga effekter på hjärta och kärl påvisas i denna modell. För att ytterligare kunna bota och lindra sjukdomssymptomen vid hjärtkärlsjukdom krävs ofta ytterligare en behandlingsform förutom blodfettssänkande medicin. Av denna anledning är det av yttersta vikt att ha relevanta musmodeller samt teknikerna för vidare utveckling av nya behandlingsstrategier mot hjärtkärlsjukdom.

ACKNOWLEDGEMENTS

Jag vill tacka följande personer som bidragit på vägen till min avhandling:

Min handledare **Li-ming Gan,** den mest effektiva människan jag känner, för din otroliga idé-rikedom, optimism och allsidighet. Du har en fantastisk förmåga att uppmuntra och inspirera mig. Tack för att du alltid tagit dig tid….särskilt om man lockar med mat eller godis ☺

Johannes Wikström, min ”jobbman” och side-kick, för att du alltid funnits vid min sida på labbet och varit mitt bollplank i diskussioner kring dessa härliga kranskärl, träning, självkänsla och bilbatterier. Det är fantastiskt att få jobba och umgås med en så positiv och humoristisk person som du! Tack för alla timmar på ultraljudslabbet och roliga konferens-resor! Jag saknar dem!

Maria Johansson, för din pedagogiska styrka och dina glada utspel vid allt ifrån seniora forskargubbar du gillar till nya klädinköp och din förmåga att få en att känna sig speciell varje gång man satte sin fot innanför dörren på Fysiologen. **Irene Andersson**, om du fanns i lyckopiller-form skulle jag börja varje dag med ett ☺. **Göran Bergström** för värdefull forskarmässig input på Fysiologen och roliga tillställningar kring ESH-möten. **Ulrika Hägg, Henrik Nyström och Evelina Bernberg** för trevliga pratstunder och diskussioner på och utanför jobbet. **Gunnel Andersson** och **Jing Jia** för fingerfärdig hjälp på labbet och trevlig sällskap. **Nina Jansson** och **Sara Roos** för ert stöd och positiva pepping varje gång vi ses på Fysiologen samt goda smak för livets njutningar utanför forskarvärlden. **Yrsa Bergmann-Sverrisdottir** för roligt resesällskap och otroligt goda middagar på din balkong. **Agneta Holmäng, Mats Jodal, Carina Mallard, Holger Nilsson, Owe Lundgren, Thomas Jansson** och **Theresa Powell** för att ni skapat en inspirerande atmosfär på Fysiologen, **Kerstin Hörnberg** för din stenkoll på allt det ekonomiska, **Arne Larsson** för all hjälp med kopierande och ditt trevliga sätt, **Lars Stage** för ditt tekniska kunnande och hjälp. **Fysiologens alla doktorander** för att vi alltid backar upp varandra i undervisningssammanhang, labbande och skrivande!

Stort tack till alla kollegor på Astra:
Ulla Brandt-Eliasson för hårt arbete, din flexiblitet och förståelse för mina humörsvängningar ☺. **Daniel Karlsson** för alla utmärkta musrakningar, scanningstimmar, ditt härliga skratt och trackande av varandras fysik. **Margareta Behrendt** för din fingerfärdighet, noggrannhet och hjälpsamhet. **Malin Palmer** för din omtanke, smittsamma skratt, ditt stöd och din humor. **Anna Ljungberg** för pepping och roligt lunchsällskap i sann Ernst-jakt-anda. **Linda Hägerstrand** för hjälp med försök, alltid med ett leende på läpparna. **Anne-Christine Andréasson** för din entusiasm när det landar nya glas på ditt skrivbord och din kunskap och snabbhet när det kommer till morfologiska färgningar. **Zsofia Berke** för ELISA analyser och trevligt samarbete. **Carl Whatling** för otroligt snabb och mycket värdefull korrektur-läsning av mina arbeten och ram. **Anders Elmgrens grupp** för stor hjälpsamhet och expertis vid alla plasma analyser. **Malin Westberg** för din koll och hjälpsamhet vid koordinerande, i princip alltid med för kort varsel.

Mina fantastiska vänner, min extra-familj i Göteborg, på Söder och över Atlanten, vad hade jag gjort utan er?
Hanna, du har förmågan att se på tillvaron med optimism och humor och jag vet inte hur ofta jag skrattar högt för mig själv åt något du sagt, gjort eller som bara du skulle förstå. Tack för alla ridturer, shoppingrundor på Bergvik, livsnödvändiga hockey-mys i bubbelkoppen och djupa diskussioner om kärlek och popcorn. **Nina,** din glada och luriga uppsyn när du är full i sjutton får mig alltid på bra humör. Du är en av de mest omtänksamma människor jag någonsin träffat! Tack för alla

boxpass, oxfilé-middagar med ”Saken är Biff”-spellista, indian-onsdagar, sparkar i baken och klappar på kinden. Kom hem snart så jag slipper vara båda rösterna i dialogen om våra upptåg! **Sara**, min forskar- och stilidol. Tack för ditt enorma stöd i livets berg-och-dal-bana. Hör ett pling i natten och läser med spänning dina sms om äventyren på McFadden, din nya klippning, alltid med katastrofal utgång eller ”Hur gör man guacemole???” Du är min livboj! **Linda,** för alla koppar te, varma scones, femrätters middagar, manikyr, pedikyr, brännboll, kubb, ordlekar, drinkar, naturistliv, uteliv, samboliv, flyttstädningar, pepptalk och sedermera härliga middagar i brasans sken i våningen. Tack för att du alltid finns vid min sida! **Stina,** för att jag fått ta del av din fantastiska man (på ett professionellt plan ☺) och för mysiga middagar, fikor och på slutet en trevlig barnpassning. **Pernilla och Martin, Elin och Niclas** för alla skratt (särskilt vid fotovisningar), otroligt vällagad mat, värmlandsförankring, ert stora stöd, medicinsk rådgivning och tillfällen att busa med ett gulligt barn ☺. **Henrik, Peter, Sibbe, Per och Pernilla, Ola och Marie, Tranan, Charlotta och Blom, Robertsson och Anna** för alla hysteriskt roliga skämt av varierad kvalite ☺, minnesvärda Danmarksresor med mustascher och 116 frukostbaguetter, midsommar-slag på Hönö, Jim Beam och UNO-spel i Falkenberg och ert enorma stöd. Love you man!

Stort tack till min nära släkt:
Mormor och morfar för er positiva anda och att ni alltid fått mig att känna mig bra, ibland kanske lite lättförtjänt ☺. Ni betyder oerhört mycket för mig! **Lena, Mats, mina kusiner Andreas och Joakim** för att ni alltid är intresserade av och nyfikna på vad jag håller på med.

Slutligen min familj:
Mamma, pappa och min syster Helena, för er kärlek och ert stöd. Tack för att ni alltid litar på att jag gör bra val för mig själv och uppmuntrar mig, fastän det inte är lätt att förstå allt ☺. Det känns tryggt att ha er med sig. Ni är bäst!

This work was supported by grants from The Swedish Medical Research Council, the Swedish Heart-Lung Foundation, AstraZeneca R&D Sweden

APPENDIX

Cardiac calculations

Left ventricular mass (LVM) = 1.05 * ((5/6 * $LV_{\text{outer area diastole SAX}}$ * $LV_{\text{length diastole LAX}}$ + $LV_{\text{wall thickness SAX}}$) – (5/6 * $LV_{\text{inner area diastole SAX}}$ * $LV_{\text{length diastole LAX}}$))

$LV_{\text{wall thickness SAX}}$ (for LVM calculations) = $(LV_{\text{outer area diastole SAX}} / \pi)^{0.5}$ – $(LV_{\text{inner area diastole SAX}} / \pi)^{0.5}$

End diastolic volume (EDV) = $LV_{\text{inner diameter diastole mmode}}^{3}$

Stroke volume (SV) = ($LV_{\text{inner diameter diastole mmode}}^{3}$ - $LV_{\text{inner diameter systole mmode}}^{3}$)

Shortening fraction (SF) = (($LV_{\text{inner diameter diastole mmode}}$ - $LV_{\text{inner diameter systole mmode}}$) / $LV_{\text{inner diameter diastole mmode}}$)) * 100

Ejection fraction (EF) = SV/ EDV * 100

Cardiac output (CO) = SV * heart rate

Coronary calculations

Coronary flow velocity reserve (CFVR):

flow velocity hyperemia / flow velocity baseline

Coronary artery flow:

LCA diameter = LCA segment area / LCA segment length

LCA area = π * (LCA diameter/2)^2

Flow (µl/min) was calculated both in baseline and in hyperemia as: (velocity time integral * LCA area * HR)

REFERENCES

1. Rosamond W, Flegal K, Friday G, Furie K, Go A, Greenlund K, Haase N, Ho M, Howard V, Kissela B, Kittner S, Lloyd-Jones D, McDermott M, Meigs J, Moy C, Nichol G, O'Donnell CJ, Roger V, Rumsfeld J, Sorlie P, Steinberger J, Thom T, Wasserthiel-Smoller S, Hong Y, for the American Heart Association Statistics Committee and Stroke Statistics Subcommittee. Heart Disease and Stroke Statistics--2007 Update: A Report From the American Heart Association Statistics Committee and Stroke Statistics Subcommittee. *Circulation.* 2007;115:e69-171.

2. Ross R, Glomset J. Atherosclerosis and the arterial smooth muscle cell: Proliferation of smooth muscle is a key event in the genesis of the lesions of atherosclerosis. *Science.* 1973;180(93):1332-1339.

3. Ross R. Atherosclerosis -- An Inflammatory Disease. *N Engl J Med.* 1999;340:115-126.

4. Ross R. The pathogenesis of atherosclerosis: a perspective for the 1990s. *Nature.* 1993;362:801.

5. Libby P. Inflammation in atherosclerosis. *Nature.* 2002;420:868-874.

6. Hansson GK. Inflammation, Atherosclerosis, and Coronary Artery Disease. *N Engl J Med.* 2005;352:1685-1695.

7. Daugherty A, Webb NR, Rateri DL, King VL. Thematic review series: The Immune System and Atherogenesis. Cytokine regulation of macrophage functions in atherogenesis. *J. Lipid Res.* 2005;46:1812-1822.

8. Fantuzzi G, Dinarello CA. Interleukin-18 and interleukin-1 beta: two cytokine substrates for ICE (caspase-1). *J Clin Immunol.* 1999;19:1-11.

9. Gracie JA, Robertson SE, McInnes IB. Interleukin-18. *J Leukoc Biol.* 2003;73:213-224.

10. Gerdes N, Sukhova GK, Libby P, Reynolds RS, Young JL, Schonbeck U. Expression of Interleukin (IL)-18 and Functional IL-18 Receptor on Human Vascular Endothelial Cells, Smooth Muscle Cells, and Macrophages: Implications for Atherogenesis. *J. Exp. Med.* 2002;195:245-257.

11. Hulthe J, McPheat W, Samnegard A, Tornvall P, Hamsten A, Eriksson P. Plasma interleukin (IL)-18 concentrations is elevated in patients with previous myocardial infarction and related to severity of coronary atherosclerosis independently of C-reactive protein and IL-6. *Atherosclerosis.* 2006;188:450.

12. Whitman SC, Ravisankar P, Daugherty A. Interleukin-18 Enhances Atherosclerosis in Apolipoprotein E-/- Mice Through Release of Interferon-{gamma}. *Circ Res.* 2002;90:e34-38.

13. Elhage R, Jawien J, Rudling M, Ljunggren H-G, Takeda K, Akira S, Bayard F, Hansson GK. Reduced atherosclerosis in interleukin-18 deficient apolipoprotein E-knockout mice. *Cardiovascular Research.* 2003;59:234.

14. Olson RE. Discovery of the Lipoproteins, Their Role in Fat Transport and Their Significance as Risk Factors. *J. Nutr.* 1998;128:439S-.

15. Segrest JP, Jones MK, De Loof H, Dashti N. Structure of apolipoprotein B-100 in low density lipoproteins. *J. Lipid Res.* 2001;42:1346-1367.

16. Brewer HB, Santamarina-Fojo S. Clinical significance of High-Density lipoproteins and the development of atherosclerosis: focus on the role of the adenosine triphosphate-Binding cassette protein A1 transporter. *The American Journal of Cardiology.* 2003;92:10-16.

17. Feher MD, Richmond W. Lipids and lipid disorders, Lippincott Williams & Wilkins. 1990.

18. Liao JK, Laufs U. Pleiotropic effects of statins. *Annu Rev Pharmacol Toxicol.* 2005;45:89-118.

19. Schachter M. Chemical, pharmacokinetic and pharmacodynamic properties of statins: an update. *Fundam Clin Pharmacol.* 2005;19:117-125.

20. Breslow J. Transgenic mouse models of lipoprotein metabolism and atherosclerosis. *PNAS.* 1993;90:8314-8318.

21. Knowles JW, Maeda N. Genetic Modifiers of Atherosclerosis in Mice. *Arterioscler Thromb Vasc Biol.* 2000;20:2336-2345.

22. Daugherty A. Mouse models of atherosclerosis. *Am J Med Sci.* 2002;323:3-10.

23. Guyton AC, Hall JE. Textbook of Medical Physiology. W.B. Saunders Company. 1998.

24. Tune JD, Gorman MW, Feigl EO. Matching coronary blood flow to myocardial oxygen consumption. *J Appl Physiol.* 2004;97:404-415.

25. Hoffman JI, Spaan JA. Pressure-flow relations in coronary circulation. *Physiol. Rev.* 1990;70:331-390.

26. Chilian WM. Coronary Microcirculation in Health and Disease: Summary of an NHLBI Workshop. *Circulation.* 1997;95:522-528.

27. Pundziute G, Schuijf JD, Jukema JW, Boersma E, de Roos A, van der Wall EE, Bax JJ. Prognostic Value of Multislice Computed Tomography Coronary Angiography in Patients With Known or Suspected Coronary Artery Disease. *Journal of the American College of Cardiology*;49:62.

28. Chatzizisis YS, Coskun AU, Jonas M, Edelman ER, Feldman CL, Stone PH. Role of Endothelial Shear Stress in the Natural History of Coronary Atherosclerosis and Vascular Remodeling: Molecular, Cellular, and Vascular Behavior. *Journal of the American College of Cardiology.* 2007;49:2379-2393.

29. Chatzizisis YS, Giannoglou GD, Parcharidis GE, Louridas GE. Is left coronary system more susceptible to atherosclerosis than right?: A pathophysiological insight. *International Journal of Cardiology.* 2007;116:7-13.

30. Meuwissen M, Siebes M, Chamuleau SA, Tijssen JG, Spaan JA, Piek JJ. Intracoronary pressure and flow velocity for hemodynamic evaluation of coronary stenoses. *Expert Review of Cardiovascular Therapy.* 2003;1:471-479.

31. Coffman JD, Gregg DE. Reactive hyperemia characteristics of the myocardium. *Am J Physiol.* 1960;199:1143-1149.

32. Strauer B. Left ventricular hypertrophy, myocardial blood flow and coronary flow reserve. *Cardiology.* 1992;81(4-5)::274-282.

33. Hozumi T, Yoshida K, Akasaka T, Asami Y, Ogata Y, Takagi T, Kaji S, Kawamoto T, Ueda Y, Morioka S. Noninvasive assessment of coronary flow velocity and coronary flow velocity reserve in the left anterior descending coronary artery by Doppler echocardiography: Comparison with invasive technique. *Journal of the American College of Cardiology.* 1998;32:1251-1259.

34. Chugh SK, Koppel J, Scott M, Shewchuk L, Goodhart D, Bonan R, Tardif JC, Worthley SG, DiMario C, Curtis MJ, Meredith IT, Anderson TJ. Coronary flow velocity reserve does not correlate with TIMI frame count in patients undergoing non-emergency percutaneous coronary intervention. *J Am Coll Cardiol.* 2004;44:778-782.

35. Vassalli G, Hess OM. Measurement of coronary flow reserve and its role in patient care. *Basic Research in Cardiology.* 1998;93:339.

36. Kozakova M, Palombo C, Pratali L, Pittella G, Galetta F, L'Abbate A. Mechanisms of Coronary Flow Reserve Impairment in Human Hypertension: An Integrated Approach by Transthoracic and Transesophageal Echocardiography. *Hypertension.* 1997;29:551-559.

37. Rim S-J, Leong-Poi H, Lindner JR, Wei K, Fisher NG, Kaul S. Decrease in Coronary Blood Flow Reserve During Hyperlipidemia Is Secondary to an Increase in Blood Viscosity. *Circulation.* 2001;104:2704-2709.

38. Tok D, Caliskan M, Gullu H, Erdogan D, Demirtas S, Muderrisoglu H. The association between hematological parameters and coronary flow reserve and coronary haemorheology in healthy subjects. *Clin Hemorheol Microcirc.* 2007;36:345-352.

39. Baller D, Notohamiprodjo G, Gleichmann U, Holzinger J, Weise R, Lehmann J. Improvement in Coronary Flow Reserve Determined by Positron Emission Tomography After 6 Months of Cholesterol-Lowering Therapy in Patients With Early Stages of Coronary Atherosclerosis. *Circulation.* 1999;99:2871-2875.

40. Fujimoto K, Hozumi T, Watanabe H, Shimada K, Takeuchi M, Sakanoue Y, Shimizu N, Ostuka R, Kawase Y, Sakamoto K, Yoshiyama M, Baba Y, Haze K, Yoshikawa J. Effect of fluvastatin therapy on coronary flow reserve in patients with hypercholesterolemia. *The American Journal of Cardiology.* 2004;93:1419-1421.

41. Hinoi T, Matsuo S, Tadehara F, Tsujiyama S, Yamakido M. Acute Effect of Atorvastatin on Coronary Circulation Measured by Transthoracic Doppler Echocardiography in Patients Without Coronary Artery Disease by Angiography. *The American journal of cardiology.* 2005;96:89-91.

42. Talukder MA, Morrison RR, Mustafa SJ. Comparison of the vascular effects of adenosine in isolated mouse heart and aorta. *Am J Physiol Heart Circ Physiol.* 2002;282:H49-57.

43. Flood A, Headrick JP. Functional characterization of coronary vascular adenosine receptors in the mouse. *Br J Pharmacol.* 2001;133:1063-1072.

44. Buus NH, Bottcher M, Hermansen F, Sander M, Nielsen TT, Mulvany MJ. Influence of Nitric Oxide Synthase and Adrenergic Inhibition on Adenosine-Induced Myocardial Hyperemia. *Circulation.* 2001;104:2305-2310.

45. Feigenbaum H. Echocardiography, Lea & Febiger. 1986.

46. Foster FS, Pavlin CJ, Harasiewicz KA, Christopher DA, Turnbull DH. Advances in ultrasound biomicroscopy. *Ultrasound in Medicine & Biology.* 2000;26:1.

47. Foster FS, Zhang MY, Zhou YQ, Liu G, Mehi J, Cherin E, Harasiewicz KA, Starkoski BG, Zan L, Knapik DA, Adamson SL. A new ultrasound instrument for in vivo microimaging of mice. *Ultrasound in Medicine & Biology.* 2002;28:1165-1172.

48. Zhou Y-Q, Foster FS, Nieman BJ, Davidson L, Chen XJ, Henkelman RM. Comprehensive transthoracic cardiac imaging in mice using ultrasound biomicroscopy with anatomical confirmation by magnetic resonance imaging. *Physiol. Genomics.* 2004:00026.02004.

49. Zhou YQ, Foster FS, Qu DW, Zhang M, Harasiewicz KA, Adamson SL. Applications for multifrequency ultrasound biomicroscopy in mice from implantation to adulthood *Physiol. Genomics.* 2002;10:113-126.

50. Ni M, Zhang M, Ding SF, Chen WQ, Zhang Y. Micro-ultrasound imaging assessment of carotid plaque characteristics in apolipoprotein-E knockout mice. *Atherosclerosis*;In Press, Corrected Proof.

51. Hockings PD, Roberts T, Galloway GJ, Reid DG, Harris DA, Vidgeon-Hart M, Groot PHE, Suckling KE, Benson GM. Repeated Three-Dimensional Magnetic Resonance Imaging of Atherosclerosis Development in Innominate Arteries of Low-Density Lipoprotein Receptor-Knockout Mice. *Circulation.* 2002;106:1716-1721.

52. McAteer MA, Schneider JE, Clarke K, Neubauer S, Channon KM, Choudhury RP. Quantification and 3D Reconstruction of Atherosclerotic Plaque Components in Apolipoprotein E Knockout Mice Using Ex Vivo High-Resolution MRI. *Arterioscler Thromb Vasc Biol.* 2004;24:2384-2390.

53. Lipinski MJ, Amirbekian V, Frias JC, Aguinaldo JG, Mani V, Briley-Saebo KC, Fuster V, Fallon JT, Fisher EA, Fayad ZA. MRI to detect atherosclerosis with gadolinium-containing immunomicelles targeting the macrophage scavenger receptor. *Magn Reson Med.* 2006;56:601-610.

54. Amirbekian V, Lipinski MJ, Briley-Saebo KC, Amirbekian S, Aguinaldo JG, Weinreb DB, Vucic E, Frias JC, Hyafil F, Mani V, Fisher EA, Fayad ZA. Detecting and assessing macrophages in vivo to evaluate atherosclerosis noninvasively using molecular MRI. *Proc Natl Acad Sci U S A.* 2007;104:961-966.

55. Wikstrom J, Gronros J, Bergstrom G, Gan L-m. Functional and Morphologic Imaging of Coronary Atherosclerosis in Living Mice

Using High-Resolution Color Doppler Echocardiography and Ultrasound Biomicroscopy. *Journal of the American College of Cardiology.* 2005;46:720-727.

56. Gronros J, Wikstrom J, Hagg U, Wandt B, Gan L-m. Proximal to Middle Left Coronary Artery Flow Velocity Ratio, As Assessed Using Color Doppler Echocardiography, Predicts Coronary Artery Atherosclerosis in Mice. *Arterioscler Thromb Vasc Biol.* 2006;26:1126-1131.

57. Gan L-m, Gronros J, Hagg U, Wikstrom J, Theodoropoulos C, Friberg P, Fritsche-Danielson R. Non-invasive real-time imaging of atherosclerosis in mice using ultrasound biomicroscopy. *Atherosclerosis.* 2007;190:313.

58. Johansson ME, Hagg U, Wikstrom J, Wickman A, Bergstrom G, Gan LM. Haemodynamically significant plaque formation and regional endothelial dysfunction in cholesterol-fed ApoE-/- mice. *Clin Sci (Lond).* 2005;108:531-538.

59. Yamashita T, Kawashima S, Ozaki M, Namiki M, Shinohara M, Inoue N, Hirata K, Umetani K, Yokoyama M. In vivo angiographic detection of vascular lesions in apolipoprotein E-knockout mice using a synchrotron radiation microangiography system. *Circ J.* 2002;66:1057-1059.

60. Caligiuri G, Levy B, Pernow J, Thoren P, Hansson GK. Myocardial infarction mediated by endothelin receptor signaling in hypercholesterolemic mice. *PNAS.* 1999;96:6920-6924.

61. Tangirala R, Rubin E, Palinski W. Quantitation of atherosclerosis in murine models: correlation between lesions in the aortic origin and in the entire aorta, and differences in the extent of lesions between sexes in LDL receptor-deficient and apolipoprotein E-deficient mice. *J. Lipid Res.* 1995;36:2320-2328.

62. Johnson J, Carson K, Williams H, Karanam S, Newby A, Angelini G, George S, Jackson C. Plaque Rupture After Short Periods of Fat Feeding in the Apolipoprotein E-Knockout Mouse: Model Characterization and Effects of Pravastatin Treatment. *Circulation.* 2005;111:1422-1430.

63. Wendelhag I, Gustavsson T, Suurküla M, Berglund G, Wikstrand J. Ultrasound measurement of wall thickness in the carotid artery: fundamental principles and description of a computerized analysing system. *Clin Physiol.* 1991;11(6):565-577.

64. Sahn DJ, DeMaria A, Kisslo J, Weyman A. Recommendations regarding quantitation in M-mode echocardiography: results of a survey of echocardiographic measurements. *Circulation.* 1978;58:1072-1083.

65. Longo MR, Guzman AW, Triebwasser JH. Normal values and commonly used echocardiographic formulae for adults. *Aviat Space Environ Med.* 1975;46:1062-1064.

66. Collins KA, Korcarz CE, Shroff SG, Bednarz JE, Fentzke RC, Lin H, Leiden JM, Lang RM. Accuracy of echocardiographic estimates of left ventricular mass in mice. *Am J Physiol Heart Circ Physiol.* 2001;280:H1954-1962.

67. Hu W, Polinsky P, Sadoun E, Rosenfeld ME, Schwartz SM. Atherosclerotic lesions in the common coronary arteries of ApoE knockout mice. *Cardiovasc Pathol.* 2005;14:120-125.

68. Wikstrom J, Gronros J, Gan L. Adenosine induces dilation of epicardial coronary arteries in mice - relationship between coronary flow velocity reserve and coronary flow reserve in vivo using transthoracic echocardiography. *Ultrasound in Medicine & Biology.* in press 2008.

69. Bradford MM. A rapid and sensitive method for the quantitation of microgram quantities of protein utilizing the principle of protein-dye binding. *Anal Biochem.* 1976;72:248-254.

70. Folch J, Lees M, Sloane Stanley GH. A simple method for the isolation and purification of total lipids from animal tissues. *J Biol Chem.* 1957;226:497-509.

71. Homan R, Anderson MK. Rapid separation and quantitation of combined neutral and polar lipid classes by high-performance liquid chromatography and evaporative light-scattering mass detection. *J Chromatogr B Biomed Sci Appl.* 1998;708:21-26.

72. Phoon CKL, Turnbull DH. Ultrasound biomicroscopy-Doppler in mouse cardiovascular development. *Physiol. Genomics.* 2003;14:3-15.

73. Summers R, Hedlund L, Cofer G. MR microscopy of the rat carotid artery after balloon injury by using an implanted imaging coil. *Magnet Reson Med.* 1995;33(6):785–789.

74. Gan LM, Wikstrom J, Bergstrom G, Wandt B. Non-invasive imaging of coronary arteries in living mice using high-resolution echocardiography. *Scand Cardiovasc J.* 2004;38:121-126.

75. Hozumi T, Yoshida K, Ogata Y, Akasaka T, Asami Y, Takagi T, Morioka S. Noninvasive Assessment of Significant Left Anterior Descending Coronary Artery Stenosis by Coronary Flow Velocity Reserve With Transthoracic Color Doppler Echocardiography. *Circulation.* 1998;97:1557-1562.

76. Saraste M, Koskenvuo J, Knuuti J, Toikka J, Laine H, Niemi P, Sakuma H, Hartiala J. Coronary flow reserve: measurement with transthoracic Doppler echocardiography is reproducible and comparable with positron emission tomography. *Clin Physiol.* 2001;21:114-122.

77. Nitenberg A, Valensi P, Sachs R, Dali M, Aptecar E, Attali J. Impairment of coronary vascular reserve and ACh-induced coronary vasodilation in diabetic patients with angiographically normal coronary arteries and normal left ventricular systolic function. *Diabetes.* 1993;42(7):1017-1025.

78. Erdogan D, Yildirim I, Ciftci O, Ozer I, Caliskan M, Gullu H, Muderrisoglu H. Effects of Normal Blood Pressure, Prehypertension, and Hypertension on Coronary Microvascular Function. *Circulation.* 2007;115:593-599.

79. Flood AJ, Willems L, Headrick JP. Coronary function and adenosine receptor-mediated responses in ischemic-reperfused mouse heart. *Cardiovascular Research.* 2002;55:161-170.

80. Godecke A, Ziegler M, Ding Z, Schrader J. Endothelial dysfunction of coronary resistance vessels in apoE-/- mice involves NO but not prostacyclin-dependent mechanisms. *Cardiovasc Res.* 2002;53:253-262.

81. Bratkovsky S, Aasum E, Birkeland CH, Riemersma RA, Myhre ES, Larsen TS. Measurement of coronary flow reserve in isolated hearts from mice. *Acta Physiol Scand.* 2004;181:167-172.

82. Faldt J, Wernstedt I, Fitzgerald SM, Wallenius K, Bergstrom G, Jansson J-O. Reduced Exercise Endurance in Interleukin-6-Deficient Mice. *Endocrinology.* 2004;145:2680-2686.

83. Staikov IN, Arnold M, Mattle HP, Remonda L, Sturzenegger M, Baumgartner RW, Schroth G. Comparison of the ECST, CC, and NASCET grading methods and ultrasound for assessing carotid stenosis. European Carotid Surgery Trial. North American Symptomatic Carotid Endarterectomy Trial. *J Neurol.* 2000;247:681-686.

84. Hozumi T, Yoshida K, Akasaka T, Asami Y, Kanzaki Y, Ueda Y, Yamamuro A, Takagi T, Yoshikawa J. Value of acceleration flow and the prestenotic to stenotic coronary flow velocity ratio by transthoracic color doppler echocardiography in noninvasive diagnosis of restenosis after percutaneous transluminal coronary angioplasty. *Journal of the American College of Cardiology.* 2000;35:164-168.

85. Saraste M, Koskenvuo JW, Mikkola J, Pelttari L, Toikka JO, Hartiala JJ. Technical achievement: transthoracic Doppler echocardiography can be used to detect LAD restenosis after coronary angioplasty. *Clin Physiol.* 2000;20:428-433.

86. Nishioka T, Kuroishi T, Sugawara Y, Yu Z, Sasano T, Endo Y, Sugawara S. Induction of serum IL-18 with Propionibacterium acnes and lipopolysaccharide in phagocytic macrophage-inactivated mice. *J Leukoc Biol.* 2007;82:327-334.

87. Wang Y-X. Cardiovascular functional phenotypes and pharmacological responses in apolipoprotein E deficient mice. *Neurobiology of Aging Developmental Origins of Aging in the Brain and Blood Vessels.* 2005;26:309-316.

88. Chen J, Li D, Schaefer RF, Mehta JL. Inhibitory effect of candesartan and rosuvastatin on CD40 and MMPs expression in apo-E knockout mice: novel insights into the role of RAS and dyslipidemia in atherogenesis. *J Cardiovasc Pharmacol.* 2004;44:446-452.

89. Wang Y-X, Martin-McNulty B, Huw L-Y, da Cunha V, Post J, Hinchman J, Vergona R, Sullivan ME, Dole W, Kauser K. Anti-atherosclerotic effect of simvastatin depends on the presence of apolipoprotein E. *Atherosclerosis.* 2002;162:23.

90. Delsing DJ, Jukema JW, van de Wiel MA, Emeis JJ, van der Laarse A, Havekes LM, Princen HM. Differential effects of amlodipine and atorvastatin treatment and their combination on atherosclerosis in ApoE*3-Leiden transgenic mice. *J Cardiovasc Pharmacol.* 2003;42:63-70.

91. Verschuren L, Kleemann R, Offerman EH, Szalai AJ, Emeis SJ, Princen HM, Kooistra T. Effect of low dose atorvastatin versus diet-induced cholesterol lowering on atherosclerotic lesion progression and inflammation in apolipoprotein E*3-Leiden transgenic mice. *Arterioscler Thromb Vasc Biol.* 2005;25:161-167.

92. Kleemann R, Princen HMG, Emeis JJ, Jukema JW, Fontijn RD, Horrevoets AJG, Kooistra T, Havekes LM. Rosuvastatin Reduces Atherosclerosis Development Beyond and Independent of Its Plasma Cholesterol-Lowering Effect in APOE*3-Leiden Transgenic Mice: Evidence for Antiinflammatory Effects of Rosuvastatin. *Circulation.* 2003;108:1368-1374.

93. Monetti M, Canavesi M, Camera M, Parente R, Paoletti R, Tremoli E, Corsini A, Bellosta S. Rosuvastatin displays anti-atherothrombotic and anti-inflammatory properties in apoE-deficient mice. *Pharmacological Research.* 2007;55:441-449.

94. Zadelaar S, Kleemann R, Verschuren L, de Vries-Van der Weij J, van der Hoorn J, Princen HM, Kooistra T. Mouse Models for Atherosclerosis and Pharmaceutical Modifiers. *Arterioscler Thromb Vasc Biol.* 2007;27:1706-1721.

95. Williams H, Johnson JL, Carson KGS, Jackson CL. Characteristics of Intact and Ruptured Atherosclerotic Plaques in Brachiocephalic Arteries of Apolipoprotein E Knockout Mice. *Arterioscler Thromb Vasc Biol.* 2002;22:788-792.